

ORIGINAL RESEARCH

Myeloid Poldip2 Contributes to the Development of Pulmonary Inflammation by Regulating Neutrophil Adhesion in a Murine Model of Acute Respiratory Distress Syndrome

Ziwei Ou, MD; Elena Dolmatova, MD; Rohan Mandavilli , BS; Hongyan Qu, MS; Georgette Gafford, PhD; Taylor White, BS; Alejandra Valdivia, PhD; Bernard Lassègue, PhD; Marina S. Hernandez , PhD; Kathy K. Griendling , PhD

BACKGROUND: Lung injury, a severe adverse outcome of lipopolysaccharide-induced acute respiratory distress syndrome, is attributed to excessive neutrophil recruitment and effector response. Poldip2 (polymerase δ -interacting protein 2) plays a critical role in regulating endothelial permeability and leukocyte recruitment in acute inflammation. Thus, we hypothesized that myeloid Poldip2 is involved in neutrophil recruitment to inflamed lungs.

METHODS AND RESULTS: After characterizing myeloid-specific *Poldip2* knockout mice, we showed that at 18 hours post-lipopolysaccharide injection, bronchoalveolar lavage from myeloid Poldip2-deficient mice contained fewer inflammatory cells (8 [4–16] versus 29 [12–57] $\times 10^4$ /mL in wild-type mice) and a smaller percentage of neutrophils (30% [28%–34%] versus 38% [33%–41%] in wild-type mice), while the main chemoattractants for neutrophils remained unaffected. In vitro, Poldip2-deficient neutrophils responded as well as wild-type neutrophils to inflammatory stimuli with respect to neutrophil extracellular trap formation, reactive oxygen species production, and induction of cytokines. However, neutrophil adherence to a tumor necrosis factor- α stimulated endothelial monolayer was inhibited by Poldip2 depletion (225 [115–272] wild-type [myePoldip2^{+/+}] versus 133 [62–178] myeloid-specific *Poldip2* knockout [myePoldip2^{-/-}] neutrophils) as was transmigration (1.7 [1.3–2.1] versus 1.1 [1.0–1.4] relative to baseline transmigration). To determine the underlying mechanism, we examined the surface expression of β 2-integrin, its binding to soluble intercellular adhesion molecule 1, and Pyk2 phosphorylation. Surface expression of β 2-integrins was not affected by Poldip2 deletion, whereas β 2-integrins and Pyk2 were less activated in Poldip2-deficient neutrophils.

CONCLUSIONS: These results suggest that myeloid Poldip2 is involved in β 2-integrin activation during the inflammatory response, which in turn mediates neutrophil-to-endothelium adhesion in lipopolysaccharide-induced acute respiratory distress syndrome.

Key Words: adhesion ■ ARDS ■ integrin ■ neutrophil ■ Poldip2

Acute respiratory distress syndrome (ARDS) is a devastating disease characterized by acute hypoxemia and non-cardiogenic pulmonary edema that often requires mechanical ventilation.¹ ARDS can

be caused by a variety of pulmonary (eg, pneumonia) or non-pulmonary (eg, sepsis, trauma, pancreatitis) insults, and therapeutic strategies are limited to the treatment of the underlying disease in conjunction with

Correspondence to: Marina Sorrentino Hernandez, PhD, Division of Cardiology, Department of Medicine, Emory University, 101 Woodruff Circle, WMB 308-C, Atlanta, GA 30322. Email: marina.sorrentino.hernandes@emory.edu

Supplemental Material for this article is available at <https://www.ahajournals.org/doi/suppl/10.1161/JAHA.121.025181>

For Sources of Funding and Disclosures, see page 14.

© 2022 The Authors. Published on behalf of the American Heart Association, Inc., by Wiley. This is an open access article under the terms of the [Creative Commons Attribution-NonCommercial-NoDerivs](https://creativecommons.org/licenses/by-nc-nd/4.0/) License, which permits use and distribution in any medium, provided the original work is properly cited, the use is non-commercial and no modifications or adaptations are made.

JAHA is available at: www.ahajournals.org/journal/jaha

CLINICAL PERSPECTIVE

What Is New?

- Myeloid-specific knockout of Poldip2 (polymerase δ -interacting protein 2) inhibits leukocyte recruitment but does not alter induction of chemokines in lung tissue during lipopolysaccharide-induced acute respiratory distress syndrome.
- Knockout of Poldip2 in neutrophils does not alter effector function or motility.
- Primed neutrophils with Poldip2 deficiency are less adhesive to endothelial cells and undergo less transmigration, likely because of reduced activation of β 2-integrins.

What Are the Clinical Implications?

- Impaired neutrophil infiltration in acute respiratory distress syndrome can be protective against lung edema and injury.
- Deficiency of myeloid Poldip2 has the potential to decrease the excessive neutrophil extravasation in sepsis-induced acute respiratory distress syndrome without affecting pathogen killing capacity.

Nonstandard Abbreviations and Acronyms

CXCL-1	chemokine (C-X-C motif) ligand 1
CXCL-2	chemokine (C-X-C motif) ligand 2
fMLP	N-Formylmethionyl-leucyl-phenylalanine
ICAM-1	intercellular adhesion molecule 1
MLMEC	mouse lung microvascular endothelial cell
NETs	neutrophil extracellular traps
PMA	phorbol 12-myristate 13-acetate
ROS	reactive oxygen species

mechanical ventilation, which itself can further damage the lungs, causing ventilator-associated lung injury.^{2,3} ARDS is characterized by increased pulmonary vascular permeability, lung edema, and loss of aerated lung tissue, as a result of an intense inflammatory response in alveoli with activation of endothelial cells and pro-coagulant processes, leukocyte and protein infiltration, and innate immune cell-mediated damage of the alveolar-capillary barriers.⁴ Such formation of alveolar protein-rich exudate is a major factor for hypoxemia and one of the earliest events that define ARDS.⁵

Neutrophils are one of the major immune cell types found in acute lung injury.⁶ In addition to their role in

the elimination of local pathogens, neutrophils can also act as a source of alveolar injury by releasing proinflammatory mediators, neutrophil extracellular traps (NETs) and reactive oxygen species (ROS).⁷ An imbalance between effective immune activation and excessive neutrophil extravasation contributes to worsening lung injury. Neutrophils enter the lung by first adhering to the activated endothelium and then exiting the microvasculature. Firm adhesion of neutrophils to the inflamed site is mediated by β 2-integrin, a leukocyte-specific integrin that binds to an α subunit and interacts with intercellular adhesion molecule-1 (ICAM-1) on the endothelium^{8,9} during leukocyte recruitment to inflamed sites.¹⁰ As a well-known regulator of cell-to-cell adhesion, β 2-integrin-dependent neutrophil adhesion in acute lung injury occurs more frequently in *Pseudomonas aeruginosa*-, immunoglobulin G immune complex- and lipopolysaccharide-induced ARDS^{9,11,12} compared with other stimuli.

We have recently focused on Poldip2 (polymerase- δ interacting protein 2) as a novel mediator of ARDS. Poldip2 is an omnipresent protein expressed in most cell types. First discovered as a DNA polymerase- δ interacting protein and a binding partner for the proliferating cell nuclear antigen,^{13,14} Poldip2 is also involved in the regulation of a number of physiological processes such as cell cycle progression, mitochondrial function, extracellular matrix deposition, focal adhesion turnover, and cell metabolism.¹⁵⁻¹⁹ In our previous studies, we showed that heterozygous Poldip2-deficient mice exhibited alleviated mortality, reduced vascular permeability, and abrogated inflammatory cytokine induction and leukocyte infiltration in both hypoxia-induced cerebral ischemia²⁰ and lipopolysaccharide-induced acute lung injury.²¹ We focused on endothelial and astrocyte Poldip2 in these reports; however, little is known about the function of Poldip2 in immune cells. In this study we used for the first time a myeloid-specific *Poldip2* knockout (*myePoldip2^{-/-}*) murine model to determine whether Poldip2 in myeloid cells, especially neutrophils, plays a role in the development of lipopolysaccharide-induced ARDS in mice. We hypothesized that loss of myeloid Poldip2 contributes to the protective phenotype of Poldip2 depletion in ARDS and investigated its potential role in neutrophil adhesion and function. We show that a major function of Poldip2 in activated neutrophils is to regulate β 2-integrin-mediated adhesion to endothelial cells, rather than other effector functions during ARDS.

METHODS

The data that support the findings of this study are available from the corresponding author upon reasonable

request. A detailed Materials and Methods section can be found in Data S1 and Table S1.

Animals

Poldip2 gene trap mice on a C57BL/6 background were previously described.²² *Poldip2* myeloid-specific knockout mice were generated by crossing a *LysM-Cre* strain (C57BL/6 background) with our newly created *Poldip2* floxed mice (C57BL/6 background).²³ Mice with *Poldip2* deficiency in myeloid cells are hereafter designated *myePoldip2*^{-/-}, while their littermates without *Poldip2* deficiency are designated *myePoldip2*^{+/+}. Hematopoiesis was evaluated by assessing complete blood counts from cardiac puncture blood samples. All animal experiments were conducted with the approval of the Institutional Animal Care and Use Committee at Emory University.

Lipopolysaccharide-Induced ARDS Model

Adult male and female (age 2.5–3.5 months) *myePoldip2*^{+/+} and *myePoldip2*^{-/-} mice were randomly divided into control and lipopolysaccharide groups. Animals in the lipopolysaccharide group received an intraperitoneal injection of lipopolysaccharide (18 mg/kg) diluted in sterile normal saline, while mice in the control group were given sterile normal saline. Eighteen hours after injection, rectal temperature was measured, and mice were euthanized by CO₂ asphyxiation for either bronchoalveolar lavage (BAL) or lung tissue collection. No difference between sexes was detected.

Bronchoalveolar Lavage

Mice were first euthanized by CO₂ inhalation and tracheas were exposed and cannulated using a 20-gauge lavage needle. For assessment of total cell counts in BAL, 3 lavages with 1 mL each of PBS containing 2 mmol/L EDTA were injected in the tracheal lavage needle and recovered as previously described.²¹ The volume recovered was measured for normalization and then centrifuged at 300g, 4 °C for 10 minutes. Pellets were resuspended in Hanks balanced salt solution without Ca²⁺ and Mg²⁺ for either total BAL cell counts or flow cytometry. For total cell counts, pellets were processed with red blood cell (RBC) lysis buffer before counting using an automated cell counter.

Flow Cytometry

For neutrophil identification in BAL, samples were processed with RBC lysis buffer and spun down at 300 g for 5 minutes at room temperature. The cell pellet was resuspended, and cells were blocked with anti-mouse CD16/32, followed by incubation with anti-mouse antibodies. For evaluation of integrin

surface expression, isolated neutrophils were labeled with eFluor450-CD11b or FITC-CD18. For evaluation of L-selectin shedding, neutrophils were stained with FITC-CD62L. Data were analyzed with Flowjo software, and leukocytes were gated as CD45⁺; myeloid cells were further gated as CD11b⁺ and neutrophils were identified as Ly6G⁺. For complete blood cell counts, white blood cell differential counting was achieved using a Hemavet 1500 blood analyzer (CDC Technologies, Oxford, CT).

Immunofluorescence, Histology, and Microscopy

Eighteen hours after PBS or lipopolysaccharide treatment, mice were euthanized using CO₂ asphyxiation, and lungs were injected with 10% formalin through the trachea. Lungs were then dissected and prepared for immunohistochemistry or immunofluorescence. Briefly, lungs were prepared for hematoxylin and eosin staining according to standard protocols.²⁴ Pictures were taken under a NanoZoomer-SQ Digital slide scanner (Hamamatsu) at 20× magnification. For immunostaining, sections were incubated with primary antibody against Ly6G and then stained with Alexa Fluor 568-conjugated secondary antibody and mounted with VECTASHIELD mounting medium with 4',6-diamidino-2-phenylindole. Pictures were taken on a Zeiss LSM 800 Airyscan microscope at 20× magnification, and the ratio of Ly6G to 4',6-diamidino-2-phenylindole positive area was calculated using ImageJ for assessment of neutrophil infiltration. Data were quantified from 3 fields of 1 section per animal, and 5 animals per group.

Bone Marrow Neutrophil Isolation

Primary bone marrow neutrophils were isolated as described²⁵ and purified by the immunomagnetic negative selection technique, using an Easysep Mouse Neutrophil Enrichment Kit (Stemcell Technologies, #19762). Neutrophil purity was always >85% and was assessed by staining with the fluorophore-labeled neutrophil marker, Ly6G, followed by flow cytometry analysis.

Cell Culture

Primary rat pulmonary microvascular endothelial cells (Cell Biologics, #RN-6011) and primary mouse lung microvascular endothelial cells (MLMECs; Cell Biologics, #C57-6011) were cultured on plates pre-coated with 0.1% gelatin. Endothelial cell medium was supplemented with 2% fetal bovine serum, endothelial cell growth factors, and antibiotics. Cells were used between passages 4–6.

Static Adhesion Assay

Isolated bone marrow neutrophils were stained with Hoechst and resuspended at 1×10^6 cells/mL. MLMECs were seeded onto a 24-well plate and treated with 10 ng/mL tumor necrosis factor- α (TNF- α) once a monolayer was formed. After 6 hours of treatment, MLMECs were washed followed by addition of bone marrow neutrophils (2×10^5 cell per well). Neutrophils and MLMECs were co-incubated for 30 minutes and then fixed using 3.7% paraformaldehyde. Fixed cells were washed and immediately imaged with an Olympus IX71 inverted fluorescent microscope using the 4',6'-diamidino-2-phenylindole fluorescence channel at 10 \times magnification. Three representative pictures were taken per well, and for each condition, triplicate wells were used. Images were analyzed with ImageJ software (National Institutes of Health); stained neutrophil nuclei were counted using the "analyze particles" module to assess firm adhesion to the MLMEC monolayer.

μ -slide Chemotaxis

μ -Slide Chemotaxis (ibidi GmbH, #80326) was used for the chemotaxis assay. Each slide contains 3 chambers, and each chamber consists of 1 channel for the cells and 2 reservoirs for the chemoattractant or chemoattractant-free media on either side of the channel. Hoechst 33342-labeled Poldip2^{+/+} and Poldip2^{+/-} bone marrow neutrophils were seeded into the central channel and exposed to N-Formylmethionyl-leucyl-phenylalanine (fMLP) (50 μ mol/L) or medium in the 2 side channels. Negative and positive control experiments were performed in the other 2 chambers of the same μ -slide. Cell movement was observed under a Leica TCS SP5 II laser scanning confocal microscope (Leica Microsystems CMS GmbH, Wetzlar, Germany). Time lapse videos were acquired using Leica Application Suite Advanced Fluorescence software with a Plan-Neo 10 \times 0.3NA air objective every minute for a total duration of 2 hours in brightfield mode and 4',6'-diamidino-2-phenylindole mode. Cell trajectories were analyzed using customized Python cell tracker software. Distance threshold was set as 30 μ m based on the cell trajectories of negative control experiments. Statistical significance ($P < 0.05$) was calculated from 3 independent experiments ($n = 3$) in which over 60 cells were evaluated in each condition per experiment.

Transmigration Assay

For the transmigration assay, 3.0 μ m pore size transwell membrane inserts were used. MLMECs (3×10^5) were seeded onto the membrane and after forming a monolayer at 24 hours, they were treated with 10 ng/mL TNF- α or media alone for 6 hours. Hoechst pre-stained neutrophils (0.5×10^6) were added to the upper chamber of each insert and 100 nmol/L fMLP or media alone was added to the lower chamber. After 2 hours of

incubation at 37 $^\circ$ C, non-migrated cells were removed from the upper surface using a wet cotton swab and migrated cells on the lower surface were fixed in 4% paraformaldehyde for 3 minutes. Inserts were then washed 3 times with PBS and membranes were removed and mounted on slides. Pictures were taken using an Olympus DP71 Digital Microscope at 10 \times and migrated neutrophils were counted by a masked observer in 6 fields for each well using ImageJ (National Institutes of Health software). Neutrophils that transmigrated into the media were also collected and counted manually using a hemocytometer.

Soluble ICAM-1 Binding Assay

The soluble ICAM-1 binding assay was used to assess beta integrin activation in neutrophils.²⁶ Bone marrow cells isolated from myePoldip2^{+/+} and myePoldip2^{+/-} mice were exposed to 2 mmol/L EDTA (as negative control), 5 mmol/L MnCl₂ or an equal volume of HBSS+, in the presence of 10 μ g/mL recombinant mouse ICAM-1-Fc chimera (R&D Systems, # 796-IC-050) and 10 μ g/mL phycoerythrin (PE)-conjugated anti-human immunoglobulin G1 Fc (ThermoFisher, #12-4998-82). Cells were fixed and then labeled with allophycocyanine-conjugated anti-Ly6G to identify neutrophils. ICAM-1 binding was measured using flow cytometry assessment of PE mean fluorescence intensity in the neutrophil subset.

SYTOX Green Assay

The SYTOX green assay was used to quantify the abundance of extracellular DNA as a surrogate of NET formation as previously described.²⁷ Poldip2^{+/+} and Poldip2^{+/-} neutrophils were isolated as described above. Fifty thousand cells per well were plated in a 96-well black clear-bottom plate and incubated at 37 $^\circ$ C for 1 hour. Cells were then stimulated with 324 nmol of phorbol 12-myristate 13-acetate or 50 μ g/mL of lipopolysaccharide. SYTOX green dye was added to each well and the fluorescence was read every 15 minutes for a total of 90 minutes at 37 $^\circ$ C. Four replicates were measured in each of 3 independent experiments. Both the time course curves as well as final fluorescence at 90 minutes were analyzed.

Reactive Oxygen Species Production

ROS production was measured using the cytochrome C assay in bone marrow neutrophils isolated from Poldip2^{+/+} and Poldip2^{+/-} mice.²⁸ Briefly, cytochrome C (100 nmol/L) was added to all wells and 25 units of superoxide dismutase was added to control wells. Neutrophils were stimulated with 100 nmol/L phorbol 12-myristate 13-acetate (PMA). Absorbance was read at 550 nm (absorbance of reduced cytochrome C) and 490 nm (to control for non-specific

absorbance) every minute for 2 hours immediately after application of phorbol 12-myristate 13-acetate. The ROS production of 3 independent experiments (2–6 independent wells each) was calculated.

RNA Extraction and Quantitative Reverse Transcription Polymerase Chain Reaction

Total RNA was purified with Qiazol (Qiagen, #79306) and the RNeasy Plus kit (Qiagen, #74104). Reverse transcription was performed using Protoscript reverse transcriptase (New England Biolabs) with random primers. The resulting cDNA was amplified with previously validated primers (Table). RPL (ribosomal protein L13A) and hypoxanthine guanine phosphoribosyl transferase were used as housekeeping genes as their expression was not affected by lipopolysaccharide treatment. Note that Poldip2 primers can detect messages transcribed from both floxed and Cre-excised alleles. Amplification was performed in 96-well plates using Forget-Me-Not EvaGreen qPCR Master Mix with low ROX (Biotium, #31045) in a QuantStudio 7 instrument (Invitrogen). Data analysis was performed using the mak3i module of the qpcR software library (version 1.4-0)^{29,30} in the R-environment.³¹

Enzyme-Linked Immunosorbent Assay

Isolated bone marrow neutrophils (3×10^6) were stimulated with lipopolysaccharide (1 $\mu\text{g/mL}$) or sterile Hanks Balanced Salt Solution with calcium and magnesium (HBSS+) for 8 hours and supernatant was then collected for TNF- α , interleukin-1 β , and interleukin-6 production measurement. Commercial ELISA kits (R&D Systems) were used according to the manufacturer’s instructions. Five independent experiments were performed, and 2 replicates were measured in each experiment.

Western Blotting

Whole cell lysate was prepared from isolated neutrophils using a lysis buffer described in our previous study.²⁰ For Pyk2 phosphorylation detection, bone marrow neutrophils were plated onto ICAM-1 coated 6-well plates and stimulated with TNF- α or media alone for the specified time. Neutrophil lysates were then prepared by adding 2 \times Laemlli buffer and boiling for 5 minutes. Samples were stored at -20°C until gel loading. Proteins were separated by SDS-PAGE, transferred to nitrocellulose membranes, and assessed by blotting with primary antibodies against Poldip2, Pyk2, phosphorylated Pyk2, β -actin and vinculin. Blots were incubated with horseradish peroxidase-conjugated secondary antibodies. Detection was performed using enhanced chemiluminescence and densitometry was performed using ImageJ.

Statistical Analysis

Analyses were performed using results from 3 to 10 independent experiments with GraphPad Prism software version 8. Data are represented as medians with their 95% CIs and analyzed using non-parametric methods, either Mann Whitney or Kruskal-Wallis with Dunnett multiple comparisons. A threshold of $P < 0.05$ was considered significant. Micrographs showing average numbers of adherent cells were selected as representative.

RESULTS

Characterization of Myeloid-Specific Poldip2 Knockout Mice

To study the effect of myeloid ablation of Poldip2 in lipopolysaccharide-induced ARDS in vivo, we established myeloid-specific *Poldip2* knockout (*myePoldip2*^{-/-}) mice by crossing a LysM-Cre strain with *Poldip2*

Table 1. Mouse Primer Sequences for RT-qPCR Assays

Annealing At 55 °C	Primer Sequences 5'-3'	
Gene	Forward	Reverse
<i>RPL</i>	ATGACAAGAAAAAGCGGATG	CTTTTCTGCCTGTTTCCGTA
<i>HPRT</i>	GCTGACCTGCTGGATTACAT	GGTCCTTTTCACCAGCAAGCT
<i>IL-1β</i>	ACCAAGCAACGACAAAATAC	CACTTTGCTCTTGACTTCTATC
<i>IL-6</i>	CTACCCCAATTTCOAATGCT	ACCACAGTGAGGAATGTCCA
<i>TNF-α</i>	CTATGTCTCAGCCTCTTCTC	GGCCATTTGGAACTTCTCA
<i>CCL-2/MCP-1</i>	CAAGATGATCCCAATGAGTAG	CAGATTTACGGGTCAACTTC
<i>CXCL-1</i>	AAAGATGCTAAAAGGTGTCC	GTATAGTGTGTGAGAAGCC
<i>CXCL-2</i>	GTTGACTTCAAGAATCCAG	CTTTCTCTTTGGTTCTTCCG
<i>Poldip2</i>	GAGACCACCGAGAATCCCG	GTGGGAATTCTGGGCTTCCCTC'

CCL-2 (also known as MCP-1 [monocyte chemoattractant protein 1]) indicates chemokine (C-C motif) ligand 2; *CXCL-1*, chemokine (C-X-C motif) ligand 1; *CXCL-2*, chemokine (C-X-C motif) ligand 2; *HPRT*, hypoxanthine guanine phosphoribosyl transferase; *IL-1 β* , interleukin-1 β ; *IL-6*, interleukin-6; *Poldip2*, polymerase (DNA-directed) δ -interacting protein 2; *RPL*, ribosomal protein L13A; RT-qPCR, quantitative reverse transcription polymerase chain reaction; and *TNF- α* , tumor necrosis factor- α .

floxed mice. To verify the efficiency and specificity of *Poldip2* deletion, we measured the expression of *Poldip2* in different organs and cells by quantitative real-time polymerase chain reaction. While *Poldip2* mRNA was decreased by 50% in purified neutrophils from *myePoldip2^{-/-}* mice compared with their littermates, *Poldip2* levels remained unchanged in hearts and lungs isolated from *myePoldip2^{-/-}* compared with *myePoldip2^{+/+}* mice (Figure 1A). Reduction of *Poldip2* protein expression in purified neutrophils was further confirmed by Western blotting (Figure 1B). To detect any potential effect of *Poldip2* myeloid-specific deletion on the composition of circulating leukocytes, we performed complete blood cell counts using a blood analyzer, and neither total leukocyte counts nor white blood cell differential counts were affected (Figure 1C). These results suggest that *Poldip2* was specifically knocked out in myeloid cells from *myePoldip2^{-/-}* mice, and that knockout efficiency was similar to *Poldip2* gene trap heterozygotes (*Poldip2^{+/-}*) (Figure S1).¹⁹ Moreover, since no change in the circulating leukocyte population was noted, *myePoldip2^{-/-}* mice are expected to possess the same numbers of defensive immune cells as wild type mice in response to external insult.

Myeloid Specific Deletion of *Poldip2* Protects Against Neutrophil Infiltration in Lipopolysaccharide-Induced ARDS

As reported in our previous research, whole body heterozygous deletion of *Poldip2* decreased lipopolysaccharide-induced mortality and immune cell recruitment into the lung.²¹ Here, we sought to explore the contribution of myeloid *Poldip2* in pulmonary leukocyte infiltration after lipopolysaccharide-induced ARDS. The development of lipopolysaccharide-induced sepsis was first confirmed by measuring rectal temperature before euthanasia. Both *myePoldip2^{+/+}* and *myePoldip2^{-/-}* mice experienced equivalent body temperature drops after lipopolysaccharide treatment indicating a similar overall response to lipopolysaccharide (Figure 2A). Leukocyte recruitment into the lung was then determined by counting cells in BAL fluid recovered 18 hours after lipopolysaccharide injection, a time point where significant accumulation of neutrophils occurs.²¹ Consistent with our results in *Poldip2* gene trap heterozygotes, lipopolysaccharide induced a remarkable increase of cell infiltration in *myePoldip2^{+/+}* mice, which was not observed in *myePoldip2^{-/-}* mice (Figure 2B). Pulmonary infiltrates in response to lipopolysaccharide in wild-type mice, but not in *myePoldip2^{-/-}* mice were further confirmed by hematoxylin and eosin staining (Figure 2C). Given that our previous study indicated that the invading myeloid cell population at 18 hours following

lipopolysaccharide-induced ARDS was mostly neutrophils,²¹ we performed flow cytometry to investigate the proportion of neutrophils in BAL leukocytes. As shown in Figure 2D and 2E, the percentage of infiltrated neutrophils was significantly reduced in *myePoldip2^{-/-}* mice after 18 hours lipopolysaccharide treatment compared with *myePoldip2^{+/+}* mice. Neutrophil infiltration into lungs was further examined by staining lungs with Ly6G, a neutrophil-specific marker. Consistent with our flow cytometry results, our immunofluorescence data suggest that the number of lung-sequestered neutrophils was significantly increased in *myePoldip2^{+/+}* mice after lipopolysaccharide and abrogated in *myePoldip2^{-/-}* mice (Figure 2F and 2G).

CXCL-1/CXCL-2 Induction In Vivo is Independent of Myeloid *Poldip2* Deletion

Because leukocyte recruitment to inflamed sites is dependent upon chemokine production by endothelium,^{32,33} we investigated the induction of major chemoattractants for neutrophils in response to lipopolysaccharide treatment in vivo by measuring their mRNA levels in lung tissue. As indicated in Figure S2, C-X-C motif ligand 1 and 2 (CXCL-1 and CXCL-2) were dramatically increased 18 hours post-lipopolysaccharide injection, in both *myePoldip2^{+/+}* mice and *myePoldip2^{-/-}* mice, but no significant difference was noted between the 2 genotypes. These findings indicate that CXCL-1/CXCL-2 production in *myePoldip2^{-/-}* mice is normal, suggesting that the primary driving force behind neutrophil recruitment to inflamed lung is not affected by depletion of *Poldip2* in myeloid cells, but there is still a possibility that other chemokines in the milieu may contribute.

Neutrophils Exhibit Normal Effector Function Ex Vivo Despite *Poldip2* Reduction

Since our data show that myeloid-specific deletion of *Poldip2* decreased lipopolysaccharide-induced neutrophil infiltration into the lungs, we next asked if *Poldip2* deletion affects neutrophil function per se. Specifically, we looked at induction of inflammatory cytokines and chemokines, as well as pathogen elimination³⁴ using freshly isolated bone marrow-derived neutrophils. Considering that *myePoldip2^{-/-}* neutrophils have a similar knockout efficiency as *Poldip2^{+/-}* mice (compare Figure S1 to Figure 1), we utilized *Poldip2^{+/-}* neutrophils as a more readily available resource for in vitro experiments. To examine the induction of inflammatory markers in response to proinflammatory stimuli, neutrophils were stimulated with lipopolysaccharide for 2 hours or 8 hours before assessing inflammatory marker mRNA or protein levels. As shown in

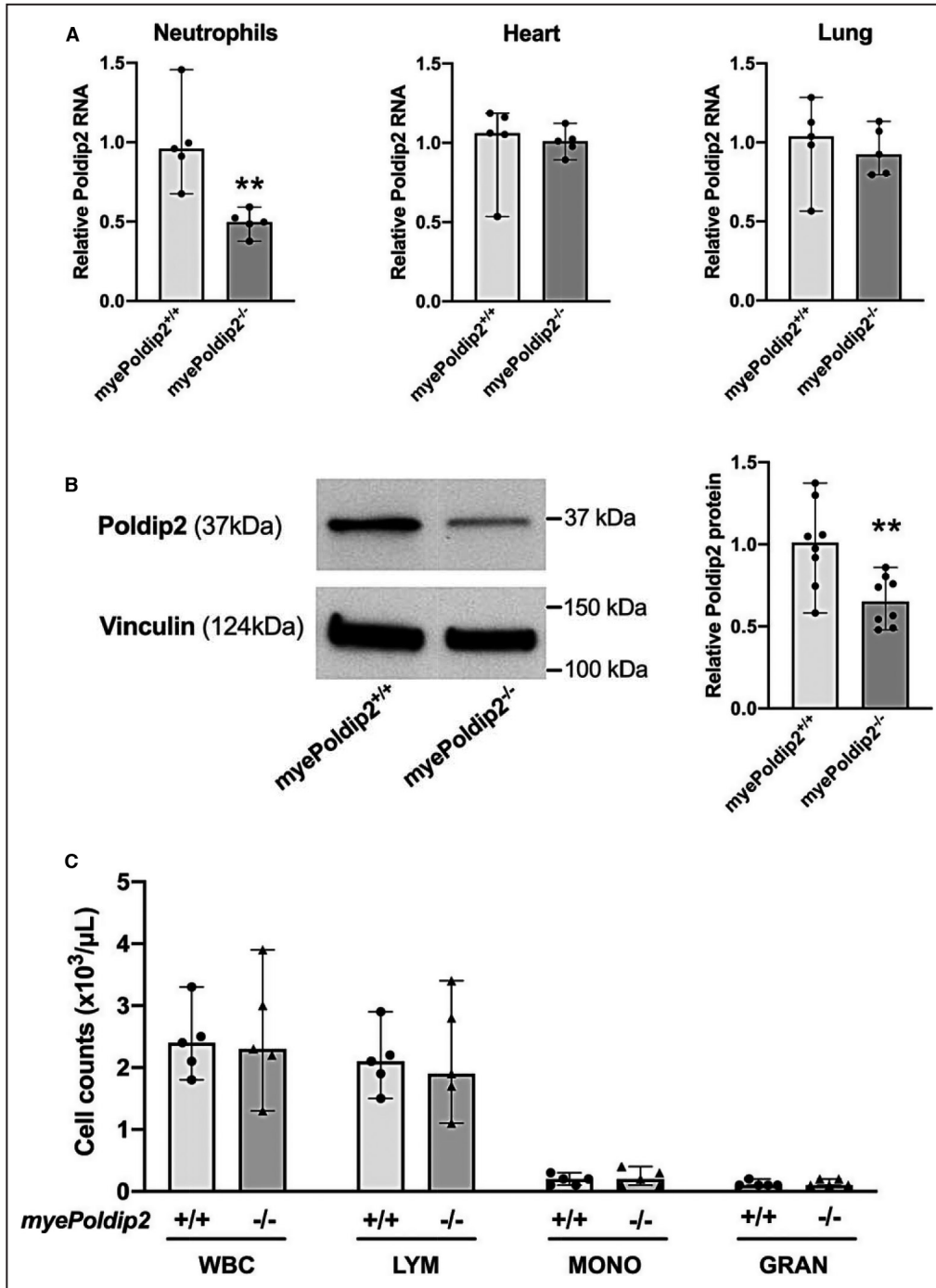


Figure 1. Characterization of myeloid-specific Poldip2 (polymerase [DNA-directed] δ -interacting protein 2) knockout mice.

A, Poldip2 mRNA expression (relative to myePoldip2^{+/+}, normalized with RPL and HPRT) in purified bone marrow neutrophils, perfused hearts and lungs, measured by quantitative reverse transcription polymerase chain reaction. Data represent medians with 95% CIs (n=5); **P<0.01 (Mann-Whitney test). **B**, Poldip2 protein expression (relative to wild-type and normalized with vinculin) in myePoldip2^{+/+} and myePoldip2^{-/-} neutrophils. Data represent medians with 95% CIs (n=8); **P<0.01 (Mann-Whitney test). **C**, Differential counts of circulating leukocytes. Blood collected from myePoldip2^{+/+} and myePoldip2^{-/-} mice was analyzed for absolute number of white blood cells, lymphocytes, monocytes, and granulocytes. Data represent medians with 95% CIs (n=5). No difference was observed between genotypes. GRAN indicates granulocytes; HPRT, hypoxanthine guanine phosphoribosyl transferase; LYM, lymphocytes; MONO, monocytes; myePoldip2^{+/+}, wild type; myePoldip2^{-/-}, myeloid-specific Poldip2 knockout; Poldip2, polymerase (DNA-directed) δ -interacting protein 2; RPL, ribosomal protein L13A; and WBC, white blood cells.

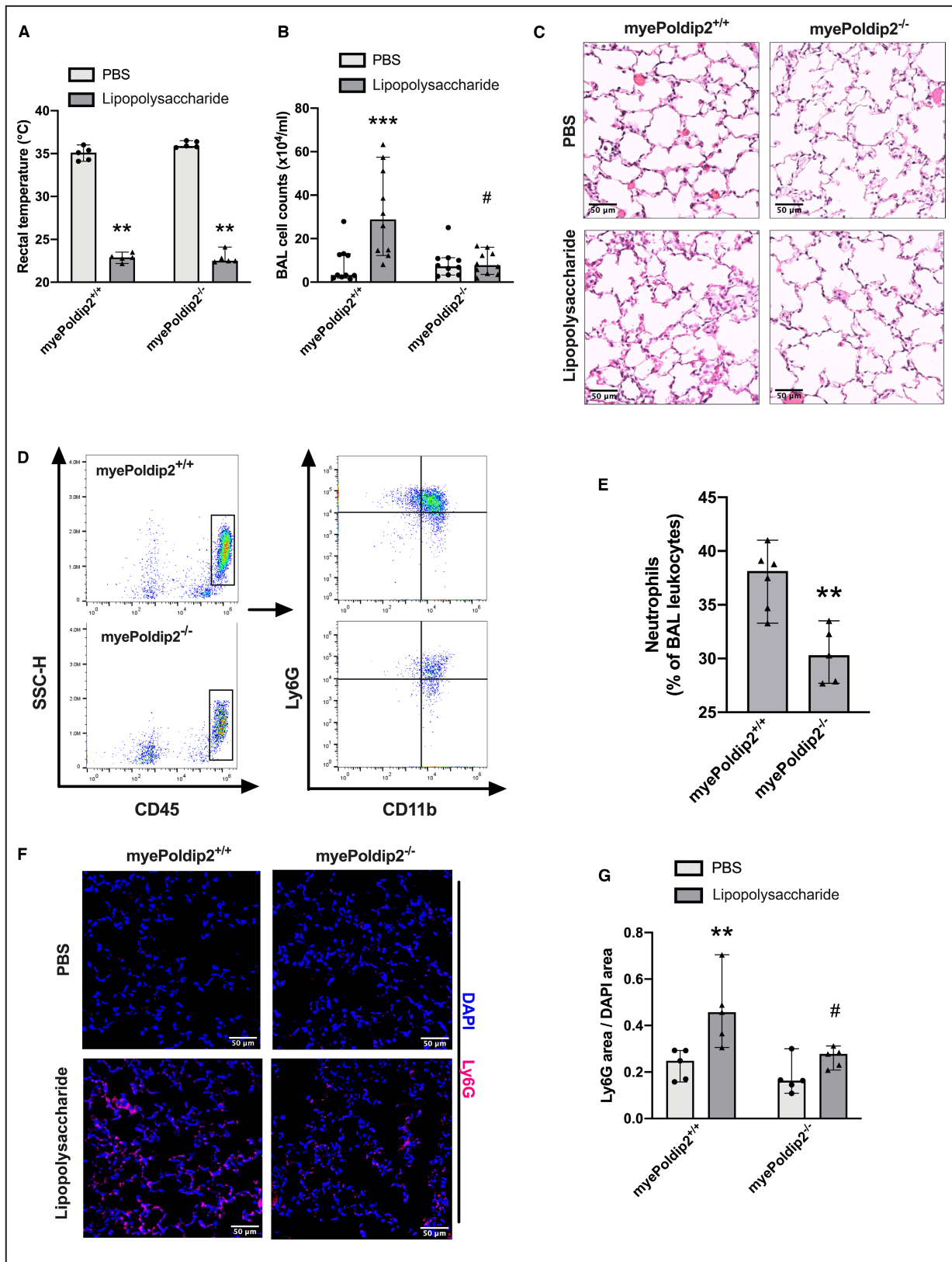


Figure 3A through 3D, inflammation-related cytokines such as TNF- α and interleukin-1 β , and neutrophil-secreted chemokine CXCL-2 (which has been shown

to be essential for diapedesis)³⁵ were increased to the same degree after lipopolysaccharide stimulation in both Poldip2^{+/+} and Poldip2^{-/-} neutrophils, with the

Figure 2. Myeloid-specific Poldip2 (polymerase [DNA-directed] δ -interacting protein 2) knockdown reduces neutrophil pulmonary infiltration in lipopolysaccharide-induced acute respiratory distress syndrome.

A, Core body temperature measured 18 hours after injection of PBS or lipopolysaccharide (18 mg/kg). Similar drops in temperature show that both genotypes responded equally to lipopolysaccharide. Data represent medians with 95% CIs (n=5); ** P <0.01 compared with PBS of the same genotype (Mann-Whitney tests). **B**, Total cell counts were measured in bronchoalveolar lavage collected 18 hours after PBS or lipopolysaccharide injection. Data represent medians with 95% CIs (n=10); *** P <0.001 compared with myePoldip2^{+/+} PBS group, # P <0.05 compared with myePoldip2^{+/+} lipopolysaccharide group (Kruskal-Wallis with Dunn multiple comparisons test). **C**, MyePoldip2^{+/+} and myePoldip2^{-/-} mice were given intraperitoneal PBS or lipopolysaccharide as described above, and lungs were harvested for hematoxylin and eosin staining. Representative pictures show decreased interstitial edema and cell infiltration in lungs after lipopolysaccharide administration in myePoldip2^{-/-} compared with myePoldip2^{+/+} (n=5). **D** and **E**, Following administration of lipopolysaccharide as above, bronchoalveolar lavage cells were labeled with CD45, CD11b, and Ly6G antibodies for neutrophil identification by flow cytometry. Panel D shows the gating strategy in which leukocytes were first gated as CD45⁺ (left) and neutrophils were further gated as CD11b⁺Ly6G⁺ (right). The percentages of neutrophils in bronchoalveolar lavage leukocytes after lipopolysaccharide injection were quantified (**E**). Data represent medians with 95% CIs (n=6 in myePoldip2^{+/+} and n=5 in myePoldip2^{-/-}); ** P <0.01 (Mann-Whitney test). **F** and **G**, Lungs were harvested 18 hours post PBS or lipopolysaccharide injection for immunofluorescence staining. Panel F shows neutrophil pulmonary infiltration after staining with the neutrophil-specific marker Ly6G, which was quantified in panel G. Data represent medians with 95% CIs (n=5); ** P <0.01 compared with myePoldip2^{+/+} PBS group, # P <0.05 compared with myePoldip2^{+/+} lipopolysaccharide group (Mann-Whitney tests). BAL indicates bronchoalveolar lavage; CD11b, integrin alpha M; CD45, leukocyte common antigen; DAPI, 4',6-diamidino-2-phenylindole; Ly6G; lymphocyte antigen 6 complex, locus G; myePoldip2^{+/+}, wild type; myePoldip2^{-/-}, myeloid-specific Poldip2 knockout; Poldip2, polymerase (DNA-directed) δ -interacting protein 2; and SSC-H, side scatter-height.

exception of interleukin-6, which was increased to a slightly lesser extent in Poldip2^{+/+}. The concentration of neutrophil-released TNF- α , interleukin-1 β and interleukin-6 in the supernatant were further measured using ELISA (Figure S3) and none of them were different between genotypes. To ascertain the ability to eliminate pathogens, we measured NETs and ROS production in Poldip2^{+/+} and Poldip2^{-/-} neutrophils in response to either PMA or lipopolysaccharide (Figure 3E and 3F and Figure S4). Poldip2^{-/-} neutrophils functioned as well as Poldip2^{+/+} neutrophils in terms of releasing pathogen killing mediators. Taken together, these data indicate that neutrophil effector functions were not disrupted by Poldip2 reduction.

Neutrophil Motility Remains Unaffected After Poldip2 Knockdown

Because mediators released by neutrophils remained intact, we next investigated whether Poldip2 would affect the ability of neutrophils to respond to chemotactic stimuli. Using a live cell imaging system, neutrophils isolated from Poldip2^{+/+} and Poldip2^{-/-} mice were placed in a channel with the general chemoattractant fMLP on 1 side, and their movement was recorded for motility analysis. As shown in Figure S5A, neutrophil speed was not affected, and total distance traveled was about the same in both genotypes (Figure S5B and Figure S6). Directional movement induced by fMLP was assessed by calculating the forward movement index, defined as the fraction of distance traveled toward fMLP. In accord with the locomotion data, neutrophil directional movement was independent of Poldip2 knockdown (Figure S5C). Altogether, these results indicated that neutrophil motility is preserved

after Poldip2 depletion and that the diminished neutrophil recruitment in inflamed lung must be due to other factors.

Poldip2 Mediates Neutrophil Adhesion to Pulmonary Endothelial Monolayer in Part Via Activation of β 2 Integrins

Leukocyte recruitment into inflamed tissue proceeds in a cascading fashion,³⁶ and a pivotal step during this process is firm adhesion of neutrophils to stimulated endothelium.^{37,38} Thus, we next sought to examine neutrophil adhesion to a pulmonary endothelial monolayer. Rat pulmonary microvascular endothelial cells were stimulated with TNF- α , one of the main effectors of lipopolysaccharide, for 6 hours before seeding neutrophils. After a 30 minute coincubation, firmly adhered neutrophils were quantified. Downregulation of Poldip2 in neutrophils isolated from myePoldip2^{-/-} mice significantly attenuated their adhesion to TNF- α -stimulated pulmonary endothelial monolayers (Figure S7). This finding was further confirmed using monolayers of MLMECs (Figure 4A and 4B). Once neutrophils adhere to endothelial cells, they migrate through the monolayer. To mimic the inflammatory microenvironment, we used a transwell system in which the insert was coated with MLMECs and stimulated with TNF- α and fMLP in the lower chamber to act as a chemoattractant. In accordance with our adhesion data, myePoldip2^{+/+} neutrophils exhibited enhanced transmigration under inflammatory conditions, which was diminished in myePoldip2^{-/-} neutrophils (Figure 4C through 4E).

To study the underlying mechanism of impaired adhesion and transmigration, we measured the surface

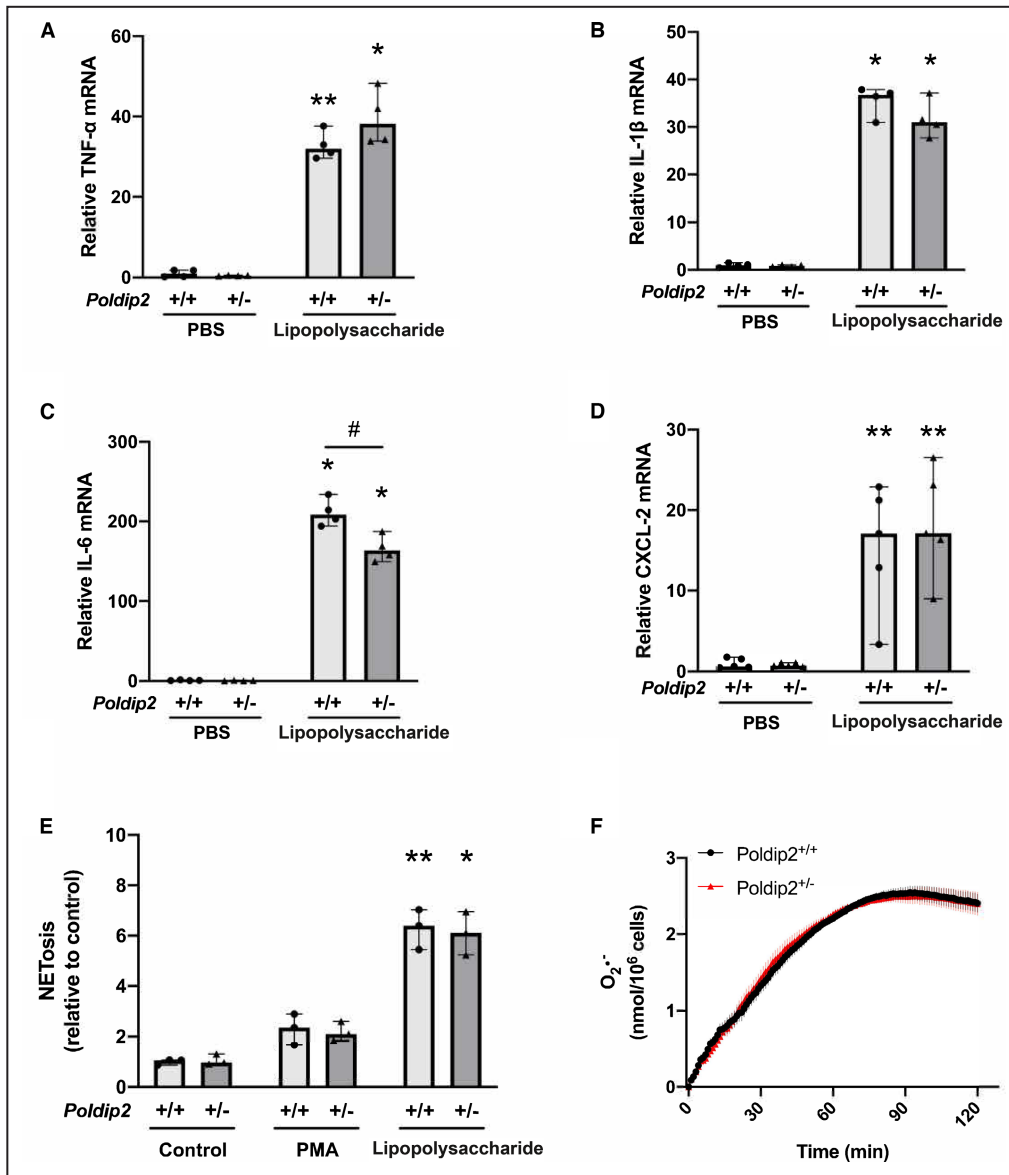
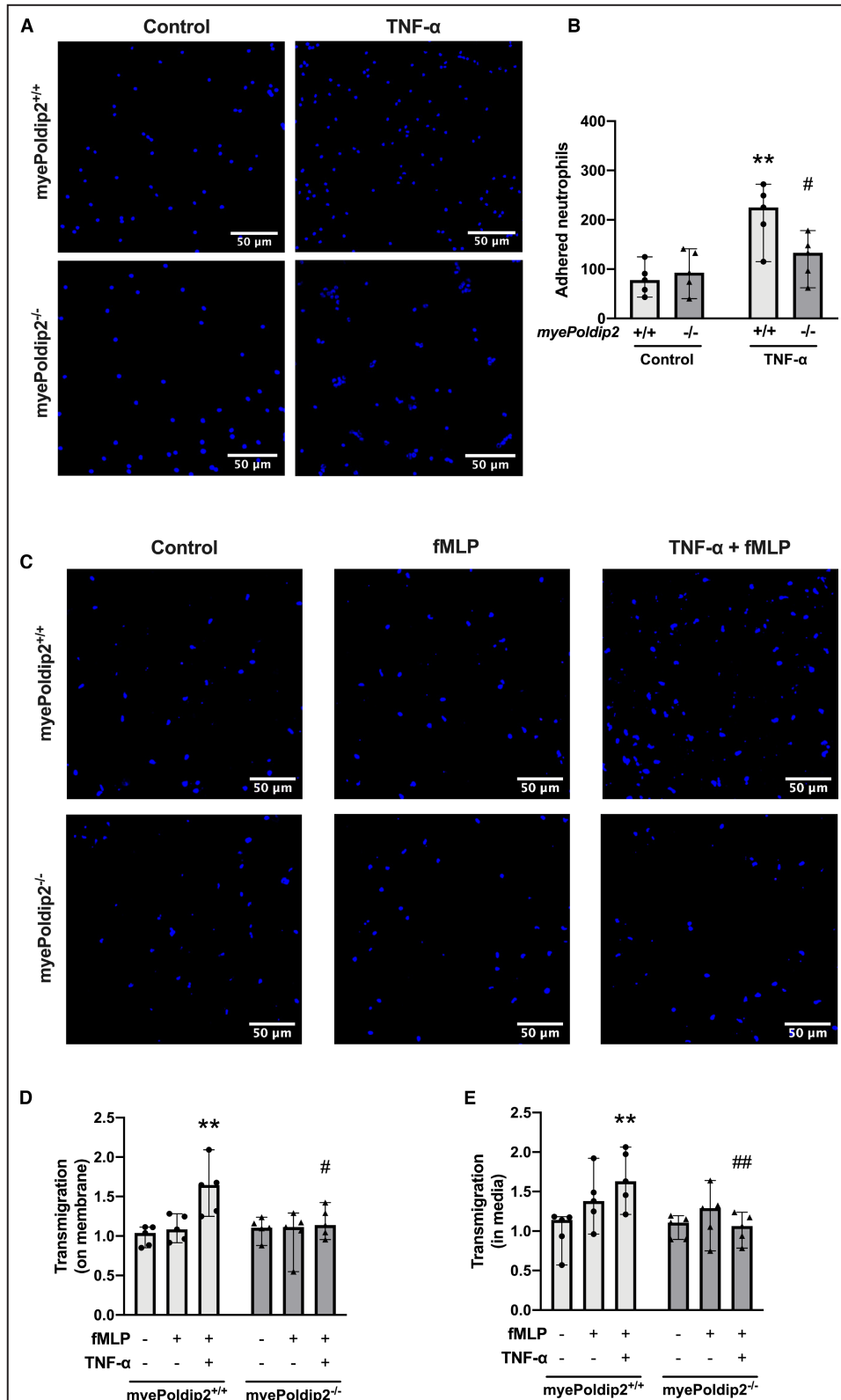


Figure 3. Poldip2 (polymerase [DNA-directed] δ -interacting protein 2) knockdown has little effect on neutrophil effector function.

A through **D**. Isolated bone marrow neutrophils were stimulated with 1 $\mu\text{g}/\text{mL}$ lipopolysaccharide for 2 hours, and mRNA expression of inflammatory markers was measured by quantitative reverse transcription polymerase chain reaction. Lipopolysaccharide induced a significant increase of TNF- α , IL-1 β , IL-6 and CXCL-2 mRNA in both Poldip2^{+/+} and Poldip2^{+/-} neutrophils. No significant difference between genotypes was noted, except that IL-6 was slightly less upregulated in Poldip2^{+/-} compared with Poldip2^{+/+} neutrophils. Bars represent medians with 95% CIs (n=4 for TNF- α , IL-1 β , and xIL-6 and n=5 for CXCL-2); * P <0.05, ** P <0.01, compared with respective PBS group; # P <0.05, compared with Poldip2^{+/+} lipopolysaccharide (Mann-Whitney tests). **E**, Isolated bone marrow neutrophils were stimulated with either PMA (324 nM) or lipopolysaccharide (50 $\mu\text{g}/\text{mL}$) before measuring neutrophil extracellular trap formation with the SYTOX green assay. Lipopolysaccharide induced a significant increase of neutrophil extracellular trap (NET) formation in both genotypes. Bars represent final fluorescence intensity at 90 minutes relative to control as medians with 95% CIs (n=3); * P <0.05, ** P <0.01, compared with respective control groups (Kruskal-Wallis with Dunn multiple comparisons test). No significant difference of NETs formation was observed between Poldip2^{+/+} and Poldip2^{+/-} neutrophils. **F**, Time course of superoxide production. Neutrophils were stimulated with PMA (324 nM) and absorbance was measured every minute for 2 hours. The concentration of superoxide was calculated as described in Methods. Data represent mean \pm SEM (n=3). No significant difference in superoxide formation was observed at any time point between Poldip2^{+/+} and Poldip2^{+/-} neutrophils. CXCL-2 indicates chemokine (C-X-C motif) ligand 2; IL-1 β interleukin-1 β ; IL-6, interleukin-6; NETosis, NET formation; PMA, phorbol 12-myristate 13-acetate; Poldip2 polymerase (DNA-directed) δ -interacting protein 2; and TNF- α , tumor necrosis factor- α .



expression of β 2 integrin, which mediates neutrophil firm adhesion.¹⁰ As expected from other studies, TNF- α triggered upregulation of both the α - and β -subunits of β 2 integrin surface expression (Figure 5A); however,

the increased expression of integrins was similar in *myePoldip2*^{-/-} and *myePoldip2*^{+/+} neutrophils. In contrast, when we assessed the *activation* of β 2 integrin by using a soluble ICAM-1 binding assay,²⁶ we found

Figure 4. Reduced adhesion and transendothelial migration in myePoldip2^{-/-} neutrophils.

A through **B**, Adhesion of Hoechst-labeled neutrophils to a TNF- α -stimulated mouse lung microvascular endothelial cell monolayer. TNF- α -induced adhesion was abrogated in neutrophils isolated from bone marrow of myePoldip2^{-/-}, compared with myePoldip2^{+/+} mice. Bars represent medians with 95% CIs (n=5); ***P*<0.01 compared with myePoldip2^{+/+} control; #*P*<0.05 compared with myePoldip2^{+/+} TNF- α (Mann-Whitney tests, 1-tailed). **C**, Representative images of neutrophils at the bottom of transwell inserts membrane following transmigration assays. **D** and **E**, Quantification of transmigrated neutrophils on the bottom of membrane (**D**) and in the lower chamber media (**E**). MyePoldip2^{+/+} neutrophils showed enhanced transmigration when the endothelial monolayer was stimulated with TNF- α and 100nM fMLP was added in the lower chamber, which was not observed in myePoldip2^{-/-} neutrophils. Data are presented as fold change relative to myePoldip2^{+/+} baseline transmigration and bars represent medians with 95% CIs (n=5); ***P*<0.01 compared with myePoldip2^{+/+} without TNF- α and fMLP, #*P*<0.05, ##*P*<0.01 compared with myePoldip2^{+/+} with TNF- α and fMLP (Mann-Whitney tests, 1-tailed). fMLP indicates N-formylmethionyl-leucyl-phenylalanine; MLMEC, mouse lung microvascular endothelial cell; myePoldip2^{+/+}, wild type; myePoldip2^{-/-}, myeloid-specific Poldip2 knockout; Poldip2, polymerase (DNA-directed) δ -interacting protein 2; and TNF- α , tumor necrosis factor α .

that TNF- α induced ICAM-1 binding in the presence of Mn²⁺ was significantly lower in myePoldip2^{-/-} neutrophils than in myePoldip2^{+/+} neutrophils (Figure 5B and 5C). The specificity of this assay for β 2 integrin was confirmed by the lack of effect of anti-Mac-1 antibody on soluble ICAM-1 binding (Figure S8). To further confirm the activation of β 2 integrin and to provide insight into how Poldip2 affected cell adhesion, we examined phosphorylation of proline-rich tyrosine kinase 2 (Pyk2), a member of the focal adhesion kinase family that is known to associate with the β 2 integrin cytoplasmic tail upon stimulation and is rapidly phosphorylated and activated in an adhesion-dependent manner.^{12,39,40} As shown in Figures 5D and 5E, Pyk2 phosphorylation was reduced in Poldip2 deficient neutrophils compared with wild-type neutrophils. These data suggest that Poldip2 is involved in the activation of β 2 integrins without disturbing integrin surface expression.

DISCUSSION

Our previous work showed that Poldip2^{-/-} mice are less susceptible to injury triggered by acute inflammation.^{20,21} However, such studies did not distinguish the role of Poldip2 in immune cells from that in endothelial cells in vivo. Here, the generation of myeloid-specific knockout mice allowed us to address the function of myeloid Poldip2 during the development of lipopolysaccharide-induced ARDS. Our findings suggest that myeloid Poldip2 is required for neutrophil recruitment in sepsis-induced ARDS, at least in part because of its role in regulating β 2-integrin activation and adhesion.

The recruitment of neutrophils into the lungs is one of the hallmarks of ARDS. Considering the destructive potential of neutrophil effectors such as NETs and ROS, delicate control of neutrophil recruitment is required to avoid severe tissue damage. Clinical data and animal models have revealed the importance of neutrophils in acute lung injury. The proportion of neutrophils in the BAL fluid correlates with ARDS severity and outcome in patients,^{41,42} and depletion of neutrophils in mice can

attenuate the severity of lung injury.⁴³ Therefore, our finding that Poldip2 levels can control neutrophil adhesion and ultimately accumulation in the lung and BAL is of utmost importance.

Lipopolysaccharide, a component of the gram-negative bacteria wall, can mimic sepsis and sequentially results indirectly in ARDS, making it a useful experimental model to study contributing mechanisms. Consistent with previous reports, we observed an obvious influx of neutrophils into the lung 18 hours post-intraperitoneal injection of lipopolysaccharide. Strikingly, we found a substantial inhibition of neutrophil sequestration and transalveolar migration in inflamed lungs in myePoldip2^{-/-} mice, supporting our hypothesis that myeloid Poldip2 is involved in the regulation of leukocyte recruitment to inflamed sites. Using this injury model, we previously found a reduction in CXCL-1 and CXCL-2 upregulation in Poldip2^{-/-} mice.²¹ However, deletion of Poldip2 only in myeloid cells led to no inhibition of these chemokines (Figure S2), suggesting that Poldip2 regulation of CXCL-1 and CXCL-2 release occurs primarily in other cell types, such as pulmonary endothelial cells and alveolar epithelial cells. Moreover, Poldip2-deficient neutrophils were able to respond normally to a chemotactic stimulus and produce equal amount of ROS and NETs. These somewhat unexpected findings led us to conclude that neutrophil Poldip2 is not involved in the ability of neutrophils to eliminate pathogens per se, but rather that it impairs the response to recruitment signals despite the presence of sufficient CXCL-1 and CXCL-2 in the milieu. It should be noted that besides these primary chemokines, there are many other chemokines that potentially contribute to leukocyte recruitment and could be affected by myeloid Poldip2 depletion, a possibility that remains to be explored. Moreover, given the fact that cytokine synthesis and secretion is a dynamic process, and the response of neutrophils to lipopolysaccharide varies over time,⁴⁴ additional time points should be studied to fully characterize the kinetics of the neutrophil response to lipopolysaccharide in myePoldip2^{-/-} mice.

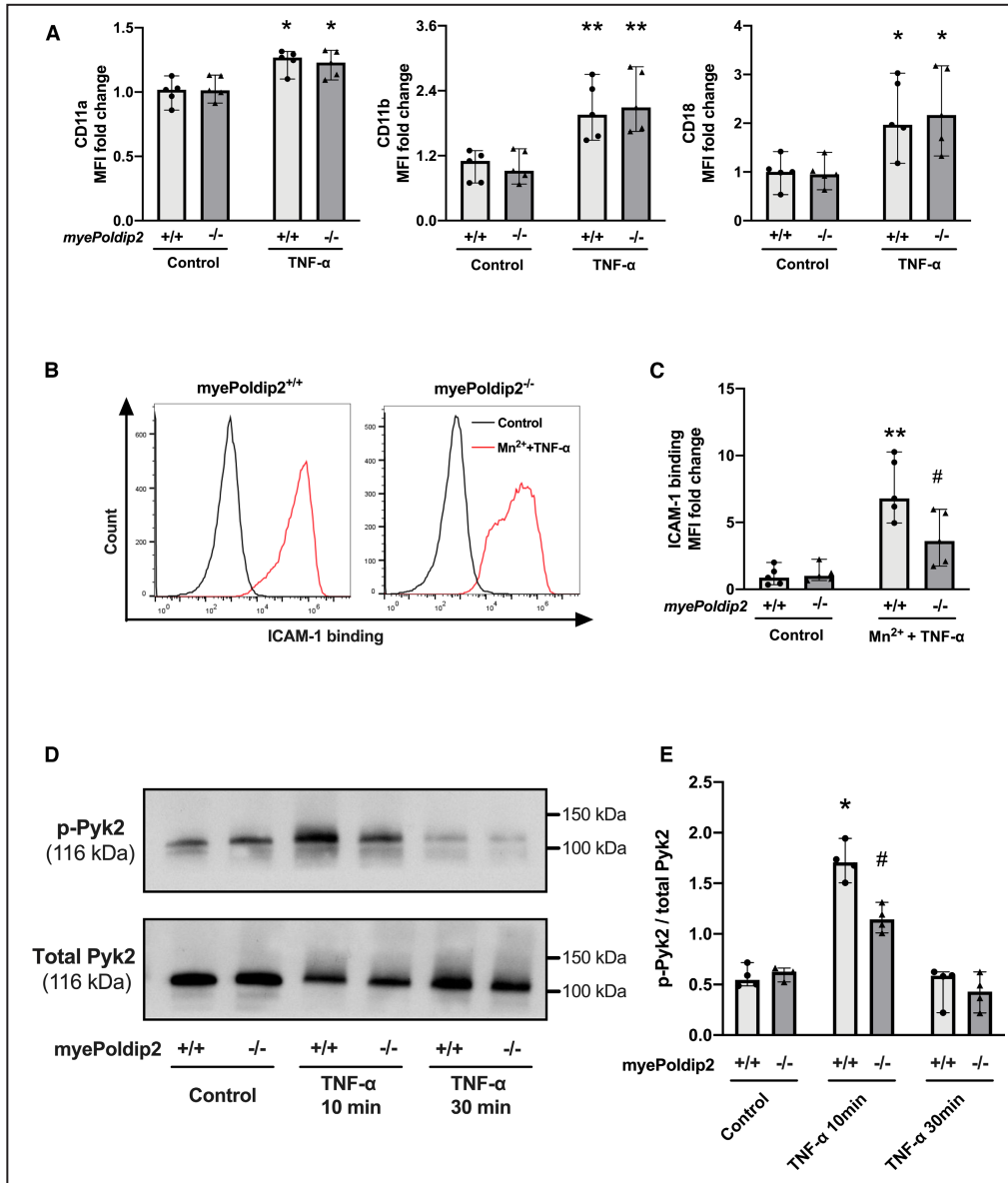


Figure 5. Poldip2 (polymerase [DNA-directed] δ -interacting protein 2) deficiency impairs β 2-integrin activation and Pyk2 phosphorylation in neutrophils.

A, Surface expression of β 2 integrin α_L subunit (left), α_M subunit (middle) and β subunit (right) in bone marrow neutrophils isolated from *myePoldip2*^{+/+} and *myePoldip2*^{-/-} mice. Data represent mean fluorescence intensity fold change relative to control as medians with 95% CIs (n=5), **P*<0.05, ***P*<0.01, compared with respective control group (Mann-Whitney tests). No significant difference was noted between genotypes. **B** and **C**, Assessment of β 2 integrin activation using the soluble intercellular adhesion molecule-1 binding assay. Isolated bone marrow neutrophils were stimulated using 20 ng/mL TNF- α for 10 minutes and incubated with soluble intercellular adhesion molecule-1-Fc in the presence of 5mM Mn²⁺. Data represent fluorescence intensity fold change as medians with 95% CIs (n=5); ***P*<0.01 compared with *myePoldip2*^{+/+} control group, #*P*<0.05 compared with *myePoldip2*^{+/+} Mn²⁺ + TNF- α group (Mann-Whitney tests). **D** and **E**, Pyk2 phosphorylation of adhered neutrophils. Isolated bone marrow neutrophils were added to intercellular adhesion molecule-1 coated plates and either left unstimulated or stimulated with 20 ng/mL TNF- α for 10 or 30 minutes. Data represent the ratio of phosphorylated Pyk2 (p-Pyk2) to total Pyk2 as medians with 95% CIs (n=4 for all groups except for *myePoldip2*^{-/-} control, in which n=3), **P*<0.05 compared with *myePoldip2*^{+/+} control group, #*P*<0.05 compared with *myePoldip2*^{+/+} TNF- α 10 minute group (Mann-Whitney tests). ICAM-1 indicates intercellular adhesion molecule 1; MFI, mean fluorescence intensity; *myePoldip2*^{+/+}, wild type; *myePoldip2*^{-/-}, myeloid-specific Poldip2 knockout; Poldip2, polymerase (DNA-directed) δ -interacting protein 2; Pyk2, protein tyrosine kinase 2 beta; and TNF- α , tumor necrosis factor α .

Leukocyte recruitment to injured tissue is an orchestrated response consisting of multiple stages and is controlled by a variety of factors.³⁷ The process of neutrophil egression from the vasculature to inflamed sites begins with their attraction by chemokine gradients, and is followed by rolling, adhesion, and transmigration at local inflamed sites.⁴⁵ L-selectin expressed by leukocytes is essential in governing leukocyte slow rolling on endothelium, and activation of neutrophils can lead to L-selectin shedding.⁴⁶ In accord with the literature, we observed a directional movement in the presence of chemoattractant fMLP as well as a downregulation of surface L-selectin (Figure S9) on neutrophils after TNF- α stimulation. However, we found that neither neutrophil motility and orientation towards fMLP nor L-selectin shedding were affected by the deficiency of Poldip2, suggesting that the impact of Poldip2 occurs primarily in subsequent stages.

Adhesion is another critical and rate-limiting step in leukocyte extravasation. Inflamed endothelial cells express adhesion molecules such as ICAM-1 to strengthen leukocyte adhesion as a consequence of their enhanced interaction.⁹ As reported in other studies, we observed an increase in neutrophil adhesion to TNF- α -stimulated pulmonary endothelial cells, but adhesion was markedly impaired in Poldip2-deficient neutrophils. Interestingly, studies have shown that neutrophils adhered to the endothelium affect the endothelial cytoskeleton, inducing remodeling of tight junctions^{47,48} and thereby increase endothelial permeability and lead to amplified neutrophil transmigration, which would be consistent with our previous observation that Poldip2 depletion reduces lung permeability.²¹ β 2-integrin on leukocytes is the counterligand to ICAM-1 on the endothelium and is pivotal in regulating leukocyte-to-endothelium adhesion.^{10,12} The strength of adhesion is determined by the amount of β 2-integrin expressed on the leukocyte surface and the status of its activation. While we found no change in surface expression of β 2-integrins, using the soluble ICAM-1 binding assay and measuring phosphorylation of the downstream effector, Pyk2, we show clear evidence of diminished β 2-integrin activation in Poldip2-deficient neutrophils.

The mechanism by which Poldip2 regulates β 2-integrin activation remains unclear. It is well-established that integrin adhesiveness is determined by both conformational change (affinity) triggered by intracellular signals and cluster formation on membrane (avidity) initiated by extracellular ligand binding.⁴⁹ β 2-integrins on leukocytes tend to be largely inactive at rest, and the switch from low-affinity to high-affinity conformation is required for ligand binding in primed neutrophils. Talin and kindlin are of great importance in mediating β 2-integrin affinity by binding to the cytoplasmic tail of the β 2 subunit.^{26,50,51} Notably, both of these molecules are cytoskeleton-associated proteins and our previous study

in vascular smooth muscle cells emphasized the significance of Poldip2 in regulating cytoskeletal dynamics,¹⁶ indicating a potential role for Poldip2 regulating inside-out β 2-integrin activation. Focal adhesion kinase is another essential protein in mediating integrin signaling and is required for ICAM-1 mediated neutrophil adhesion.⁵² Intriguingly, our team found that Poldip2 is involved with focal adhesion kinase activation in both endothelial cells and smooth muscle cells,^{15,20} which potentially implicates a similar pathway in leukocytes. Our current study extends these findings to include Pyk2, a focal adhesion kinase family member. Finally, Poldip2 depletion was shown to upregulate the expression of β 1-integrin in smooth muscle cells as a result of elevated activation of the PI3K/Akt/mTOR signaling pathway,⁵³ suggesting that while regulation of integrin signaling may be a common mechanism for Poldip2-mediated effects, the precise pathways affecting different integrins may be cell type-specific. Further work will be required to define how Poldip2 regulates β 2-integrin activity in neutrophils.

In summary, our work indicates that Poldip2 mediates β 2-integrin-dependent adhesion at least in part by impacting β 2-integrin activation during neutrophil recruitment to inflamed lungs but is unrelated to their effector response to inflammatory stimuli. Together with our previous studies delineating a role for Poldip2 in endothelial permeability and inflammation, these findings suggest that Poldip2 may play a central role in the response to lung injury.

ARTICLE INFORMATION

Received December 24, 2021; accepted March 31, 2022.

Affiliations

Division of Cardiology, Department of Medicine, Emory University, Atlanta, GA (Z.O., E.D., R.M., H.Q., G.G., T.W., A.V., B.L., M.S.H., K.K.G.); and Department of Cardiovascular Medicine, Xiangya Hospital, Central South University, Changsha, China (Z.O.).

Acknowledgments

Z.O. is a member of the joint training program between Emory University School of Medicine and Xiangya School of Medicine, Central South University, and is supported by the China Scholarship Council. We would like to thank Rebecca Zhang from the Data Analytics and Biostatistics Core of the Emory Department of Medicine for help with statistics, Hassan Sellak for help with complete blood count, Kimberly Cooney for useful information on NETs formation, Giji Joseph for help with immunohistochemistry, and Steven Forrester for the customized cell tracking software.

Sources of Funding

This study was supported in part by the Emory Flow Cytometry Core, one of the Emory Integrated Core Facilities and is subsidized by the Emory University School of Medicine. This work was supported by National Institutes of Health grants and HL152167 and HL095070 to Kathy K. Griendling and HL151133 to Elena Dolmatova.

Disclosures

None.

Supplemental Material

Data S1
Table S1
Figures S1–S9

REFERENCES

- Matthay MA, Zemans RL, Zimmerman GA, Arabi YM, Beitler JR, Mercat A, Herridge M, Randolph AG, Calfee CS. Acute respiratory distress syndrome. *Nat Rev Dis Primers*. 2019;5:18. doi: [10.1038/s41572-019-0069-0](https://doi.org/10.1038/s41572-019-0069-0)
- Ragaller M, Richter T. Acute lung injury and acute respiratory distress syndrome. *J Emerg Trauma Shock*. 2010;3:43–51. doi: [10.4103/0974-2700.58663](https://doi.org/10.4103/0974-2700.58663)
- Fan E, Brodie D, Slutsky AS. Acute respiratory distress syndrome: advances in diagnosis and treatment. *JAMA*. 2018;319:698–710. doi: [10.1001/jama.2017.21907](https://doi.org/10.1001/jama.2017.21907)
- Thompson BT, Chambers RC, Liu KD. Acute respiratory distress syndrome. *N Engl J Med*. 2017;377:1904–1905. doi: [10.1056/NEJMra1608077](https://doi.org/10.1056/NEJMra1608077)
- Herrero R, Sanchez G, Lorente JA. New insights into the mechanisms of pulmonary edema in acute lung injury. *Ann Transl Med*. 2018;6:32. doi: [10.21037/atm.2017.12.18](https://doi.org/10.21037/atm.2017.12.18)
- Grommes J, Soehnlein O. Contribution of neutrophils to acute lung injury. *Mol Med*. 2011;17:293–307. doi: [10.2119/molmed.2010.00138](https://doi.org/10.2119/molmed.2010.00138)
- Mantovani A, Cassatella MA, Costantini C, Jaillon S. Neutrophils in the activation and regulation of innate and adaptive immunity. *Nat Rev Immunol*. 2011;11:519–531. doi: [10.1038/nri3024](https://doi.org/10.1038/nri3024)
- Doerschuk CM, Quinlan WM, Doyle NA, Bullard DC, Vestweber D, Jones ML, Takei F, Ward PA, Beaudet AL. The role of P-selectin and ICAM-1 in acute lung injury as determined using blocking antibodies and mutant mice. *J Immunol*. 1996;157:4609–4614.
- Moreland JG, Fuhrman RM, Pruessner JA, Schwartz DA. CD11b and intercellular adhesion molecule-1 are involved in pulmonary neutrophil recruitment in lipopolysaccharide-induced airway disease. *Am J Respir Cell Mol Biol*. 2002;27:474–480. doi: [10.1165/rcmb.4694](https://doi.org/10.1165/rcmb.4694)
- Yuki K, Hou L. Role of $\beta 2$ integrins in neutrophils and sepsis. *Infect Immun*. 2020;88:e00031-20. doi: [10.1128/IAI.00031-20](https://doi.org/10.1128/IAI.00031-20)
- Mulligan MS, Varani J, Warren JS, Till GO, Smith CW, Anderson DC, Todd RF III, Ward PA. Roles of beta 2 integrins of rat neutrophils in complement- and oxygen radical-mediated acute inflammatory injury. *J Immunol*. 1992;148:1847–1857.
- Xu J, Gao XP, Ramchandran R, Zhao YY, Vogel SM, Malik AB. Nonmuscle myosin light-chain kinase mediates neutrophil transmigration in sepsis-induced lung inflammation by activating beta2 integrins. *Nat Immunol*. 2008;9:880–886. doi: [10.1038/ni.1628](https://doi.org/10.1038/ni.1628)
- Liu L, Rodriguez-Belmonte EM, Mazloum N, Xie B, Lee MY. Identification of a novel protein, PDIP38, that interacts with the p50 subunit of DNA polymerase delta and proliferating cell nuclear antigen. *J Biol Chem*. 2003;278:10041–10047. doi: [10.1074/jbc.M208694200](https://doi.org/10.1074/jbc.M208694200)
- Xie B, Li H, Wang Q, Xie S, Rahmeh A, Dai W, Lee MY. Further characterization of human DNA polymerase delta interacting protein 38. *J Biol Chem*. 2005;280:22375–22384. doi: [10.1074/jbc.M414597200](https://doi.org/10.1074/jbc.M414597200)
- Datta SR, McGrail DJ, Vukelic S, Huff LP, Lyle AN, Pounkova L, Lee M, Seidel-Rogol B, Khalil MK, Hilenski LL, et al. Poldip2 controls vascular smooth muscle cell migration by regulating focal adhesion turnover and force polarization. *Am J Physiol Heart Circ Physiol*. 2014;307:H945–H957. doi: [10.1152/ajpheart.00918.2013](https://doi.org/10.1152/ajpheart.00918.2013)
- Lyle AN, Deshpande NN, Taniyama Y, Seidel-Rogol B, Pounkova L, Du P, Papaharalambus C, Lassegue B, Griendling KK. Poldip2, a novel regulator of Nox4 and cytoskeletal integrity in vascular smooth muscle cells. *Circ Res*. 2009;105:249–259. doi: [10.1161/CIRCRESAHA.109.193722](https://doi.org/10.1161/CIRCRESAHA.109.193722)
- Matsushima S, Zablocki D, Tsutsui H, Sadoshima J. Poldip2 negatively regulates matrix synthesis at focal adhesions. *J Mol Cell Cardiol*. 2016;94:10–12. doi: [10.1016/j.jmcc.2016.03.001](https://doi.org/10.1016/j.jmcc.2016.03.001)
- Paredes F, Sheldon K, Lassegue B, Williams HC, Faidley EA, Benavides GA, Torres G, Sanhueza-Olivares F, Yeligar SM, Griendling KK, et al. Poldip2 is an oxygen-sensitive protein that controls PDH and alphaK-GDH lipoylation and activation to support metabolic adaptation in hypoxia and cancer. *Proc Natl Acad Sci USA*. 2018;115:1789–1794.
- Sutliff RL, Hilenski LL, Amanso AM, Parastatidis I, Dikalova AE, Hansen L, Datta SR, Long JS, El-Ali AM, Joseph G, et al. Polymerase delta interacting protein 2 sustains vascular structure and function. *Arterioscler Thromb Vasc Biol*. 2013;33:2154–2161. doi: [10.1161/ATVBAHA.113.301913](https://doi.org/10.1161/ATVBAHA.113.301913)
- Eidson LN, Gao Q, Qu H, Kikuchi DS, Campos ACP, Faidley EA, Sun Y-Y, Kuan C-Y, Pagano RL, Lassegue B, et al. Poldip2 controls leukocyte infiltration into the ischemic brain by regulating focal adhesion kinase-mediated VCAM-1 induction. *Sci Rep*. 2021;11:5533. doi: [10.1038/s41598-021-84987-z](https://doi.org/10.1038/s41598-021-84987-z)
- Forrester SJ, Xu Q, Kikuchi DS, Okwan-Duodu D, Campos AC, Faidley EA, Zhang G, Lassegue B, Sadikot RT, Griendling KK, et al. Poldip2 deficiency protects against lung edema and vascular inflammation in a model of acute respiratory distress syndrome. *Clin Sci (Lond)*. 2019;133:321–334. doi: [10.1042/CS20180944](https://doi.org/10.1042/CS20180944)
- Brown DI, Lassegue B, Lee M, Zafari R, Long JS, Saavedra HI, Griendling KK. Poldip2 knockout results in perinatal lethality, reduced cellular growth and increased autophagy of mouse embryonic fibroblasts. *PLoS One*. 2014;9:e96657. doi: [10.1371/journal.pone.0096657](https://doi.org/10.1371/journal.pone.0096657)
- Lassegue B, Kumar S, Mandavilli R, Wang K, Tsai M, Kang D-W, Demos C, Hernandez MS, San Martin A, Taylor WR, et al. Characterization of Poldip2 knockout mice: avoiding incorrect gene targeting. *PLoS One*. 2021;16:e0247261. doi: [10.1371/journal.pone.0247261](https://doi.org/10.1371/journal.pone.0247261)
- Gandjeva A, Tuder RM. Lung histological methods. *Methods Mol Biol*. 2018;1809:315–329. doi: [10.1007/978-1-4939-8570-8_20](https://doi.org/10.1007/978-1-4939-8570-8_20)
- Amend SR, Valkenburg KC, Pienta KJ. Murine hind limb long bone dissection and bone marrow isolation. *J Vis Exp*. 2016. doi: [10.3791/53936](https://doi.org/10.3791/53936)
- Lefort CT, Rossaint J, Moser M, Petrich BG, Zarbock A, Monkley SJ, Critchley DR, Ginsberg MH, Fassler R, Ley K. Distinct roles for talin-1 and kindlin-3 in LFA-1 extension and affinity regulation. *Blood*. 2012;119:4275–4282. doi: [10.1182/blood-2011-08-373118](https://doi.org/10.1182/blood-2011-08-373118)
- Xu K, Cooney KA, Shin EY, Wang L, Deppen JN, Ginn SC, Levit RD. Adenosine from a biologic source regulates neutrophil extracellular traps (NETs). *J Leukoc Biol*. 2019;105:1225–1234. doi: [10.1002/JLB.3VMA0918-374R](https://doi.org/10.1002/JLB.3VMA0918-374R)
- Miller FJ Jr, Griendling KK. Functional evaluation of nonphagocytic NAD(P)H oxidases. *Methods Enzymol*. 2002;353:220–233. doi: [10.1016/s0076-6879\(02\)53050-0](https://doi.org/10.1016/s0076-6879(02)53050-0)
- Boggy GJ, Woolf PJ. A mechanistic model of PCR for accurate quantification of quantitative PCR data. *PLoS One*. 2010;5:e12355. doi: [10.1371/journal.pone.0012355](https://doi.org/10.1371/journal.pone.0012355)
- Ritz C, Spiess AN. qpcR: an R package for sigmoidal model selection in quantitative real-time polymerase chain reaction analysis. *Bioinformatics*. 2008;24:1549–1551. doi: [10.1093/bioinformatics/btn227](https://doi.org/10.1093/bioinformatics/btn227)
- R Core Team. *R: A language and environment for statistical computing*. Vienna, Austria: R Foundation for Statistical Computing; 2018.
- Capucetti A, Albano F, Bonecchi R. Multiple roles for chemokines in neutrophil biology. *Front Immunol*. 2020;11:259. doi: [10.3389/fimmu.2020.01259](https://doi.org/10.3389/fimmu.2020.01259)
- Kim ND, Luster AD. The role of tissue resident cells in neutrophil recruitment. *Trends Immunol*. 2015;36:547–555. doi: [10.1016/j.it.2015.07.007](https://doi.org/10.1016/j.it.2015.07.007)
- Mayadas TN, Cullere X, Lowell CA. The multifaceted functions of neutrophils. *Annu Rev Pathol*. 2014;9:181–218. doi: [10.1146/annurev-pathol-1-020712-164023](https://doi.org/10.1146/annurev-pathol-1-020712-164023)
- Giribi T, Lenn T, Perez L, Rolas L, Barkaway A, Thiriot A, del Fresno C, Lynam E, Hub E, Thelen M, et al. Distinct compartmentalization of the chemokines CXCL1 and CXCL2 and the atypical receptor ACKR1 determine discrete stages of neutrophil diapedesis. *Immunity*. 2018;49:1062–1076.e1066. doi: [10.1016/j.immuni.2018.09.018](https://doi.org/10.1016/j.immuni.2018.09.018)
- Kelly M, Hwang JM, Kuberski P. Modulating leukocyte recruitment in inflammation. *J Allergy Clin Immunol*. 2007;120:3–10. doi: [10.1016/j.jaci.2007.05.017](https://doi.org/10.1016/j.jaci.2007.05.017)
- Muller WA. Leukocyte-endothelial-cell interactions in leukocyte transmigration and the inflammatory response. *Trends Immunol*. 2003;24:327–334. doi: [10.1016/S1471-4906\(03\)00117-0](https://doi.org/10.1016/S1471-4906(03)00117-0)
- Wilhelmsen K, Farrar K, Hellman J. Quantitative in vitro assay to measure neutrophil adhesion to activated primary human microvascular endothelial cells under static conditions. *J Vis Exp*. 2013:e50677. doi: [10.3791/50677](https://doi.org/10.3791/50677)
- Yan SR, Novak MJ. Beta2 integrin-dependent phosphorylation of protein-tyrosine kinase Pyk2 stimulated by tumor necrosis factor alpha and fMLP in human neutrophils adherent to fibrinogen. *FEBS Lett*. 1999;451:33–38.
- Miura Y, Tohyama Y, Hishita T, Lala A, De Nardin E, Yoshida Y, Yamamura H, Uchiyama T, Tohyama K. Pyk2 and Syk participate in functional activation of granulocytic HL-60 cells in a different manner. *Blood*. 2000;96:1733–1739. doi: [10.1182/blood.V96.5.1733](https://doi.org/10.1182/blood.V96.5.1733)
- Parsons PE, Fowler AA, Hyers TM, Henson PM. Chemotactic activity in bronchoalveolar lavage fluid from patients with adult respiratory distress syndrome. *Am Rev Respir Dis*. 1985;132:490–493.
- Steinberg KP, Milberg JA, Martin TR, Maunder RJ, Cockrill BA, Hudson LD. Evolution of bronchoalveolar cell populations in the adult respiratory distress syndrome. *Am J Respir Crit Care Med*. 1994;150:113–122. doi: [10.1164/ajrccm.150.1.8025736](https://doi.org/10.1164/ajrccm.150.1.8025736)

43. Abraham E, Carmody A, Shenkar R, Arcaroli J. Neutrophils as early immunologic effectors in hemorrhage- or endotoxemia-induced acute lung injury. *Am J Physiol Lung Cell Mol Physiol*. 2000;279:L1137–L1145. doi: [10.1152/ajplung.2000.279.6.L1137](https://doi.org/10.1152/ajplung.2000.279.6.L1137)
44. Naegelen I, Beaume N, Plancon S, Schenten V, Tschirhart EJ, Brechard S. Regulation of neutrophil degranulation and cytokine secretion: a novel model approach based on linear fitting. *J Immunol Res*. 2015;2015:1–15. doi: [10.1155/2015/817038](https://doi.org/10.1155/2015/817038)
45. Middleton J, Patterson AM, Gardner L, Schmutz C, Ashton BA. Leukocyte extravasation: chemokine transport and presentation by the endothelium. *Blood*. 2002;100:3853–3860. doi: [10.1182/blood.V100.12.3853](https://doi.org/10.1182/blood.V100.12.3853)
46. Hafezi-Moghadam A, Thomas KL, Prorock AJ, Huo Y, Ley K. L-selectin shedding regulates leukocyte recruitment. *J Exp Med*. 2001;193:863–872. doi: [10.1084/jem.193.7.863](https://doi.org/10.1084/jem.193.7.863)
47. Furuse M, Itoh M, Hirase T, Nagafuchi A, Yonemura S, Tsukita S, Tsukita S. Direct association of occludin with ZO-1 and its possible involvement in the localization of occludin at tight junctions. *J Cell Biol*. 1994;127:1617–1626. doi: [10.1083/jcb.127.6.1617](https://doi.org/10.1083/jcb.127.6.1617)
48. Su WH, Chen HI, Jen CJ. Differential movements of VE-cadherin and PECAM-1 during transmigration of polymorphonuclear leukocytes through human umbilical vein endothelium. *Blood*. 2002;100:3597–3603. doi: [10.1182/blood-2002-01-0303](https://doi.org/10.1182/blood-2002-01-0303)
49. Stewart M, Hogg N. Regulation of leukocyte integrin function: affinity vs. avidity. *J Cell Biochem*. 1996;61:554–561. doi: [10.1002/\(SICI\)1097-4644\(19960616\)61:4<554::AID-JCB8>3.0.CO;2-N](https://doi.org/10.1002/(SICI)1097-4644(19960616)61:4<554::AID-JCB8>3.0.CO;2-N)
50. Tadokoro S, Shattil SJ, Eto K, Tai V, Liddington RC, de Pereda JM, Ginsberg MH, Calderwood DA. Talin binding to integrin beta tails: a final common step in integrin activation. *Science*. 2003;302:103–106. doi: [10.1126/science.1086652](https://doi.org/10.1126/science.1086652)
51. Moser M, Nieswandt B, Ussar S, Pozgajova M, Fassler R. Kindlin-3 is essential for integrin activation and platelet aggregation. *Nat Med*. 2008;14:325–330. doi: [10.1038/nm1722](https://doi.org/10.1038/nm1722)
52. Kasorn A, Alcaide P, Jia Y, Subramanian KK, Sarraj B, Li Y, Loison F, Hattori H, Silberstein LE, Lusinskas WF, et al. Focal adhesion kinase regulates pathogen-killing capability and life span of neutrophils via mediating both adhesion-dependent and -independent cellular signals. *J Immunol*. 2009;183:1032–1043. doi: [10.4049/jimmunol.0802984](https://doi.org/10.4049/jimmunol.0802984)
53. Fujii M, Amanso A, Abrahao TB, Lassegue B, Griendling KK. Polymerase delta-interacting protein 2 regulates collagen accumulation via activation of the Akt/mTOR pathway in vascular smooth muscle cells. *J Mol Cell Cardiol*. 2016;92:21–29. doi: [10.1016/j.yjmcc.2016.01.016](https://doi.org/10.1016/j.yjmcc.2016.01.016)

SUPPLEMENTAL MATERIAL

Data S1.

Supplemental Methods

Animals

Poldip2 gene trap mice on a C57BL/6 background were produced by the Texas A&M Institute for Genomic Medicine. Since homozygous Poldip2 depletion in gene trap mice is embryonically lethal,²² heterozygous Poldip2-deficient mice (Poldip2^{+/-}) were used in this study, and wild-type mice (Poldip2^{+/+}) were used as controls. Poldip2 myeloid specific knockout mice were generated by crossing a LysM-Cre strain (C57BL/6 background) obtained from The Jackson Laboratory with our newly created Poldip2 floxed mice (C57BL/6 background).²³ Mice with Poldip2 deficiency in myeloid cells are hereafter designated myePoldip2^{-/-}, while their littermates without Poldip2 deficiency are designated myePoldip2^{+/+}. Mice were genotyped for Cre using a real-time PCR assay with melting curve analysis from The Jackson Laboratory and for floxed Poldip2 using a standard three-primer PCR method.²³ Hematopoiesis of these genetic modified mice was evaluated by assessing complete blood count from cardiac puncture blood samples. Mice received LabDiet chow 5053 and water ad libitum. All animal experiments were conducted with the approval of the Institutional Animal Care and Use Committee at Emory University.

LPS-induced ARDS model

Adult male and female (age 2.5-3.5 months) myePoldip2^{+/+} and myePoldip2^{-/-} mice were randomly divided into control and LPS groups using the block randomization method. Animals in the LPS group received an intraperitoneal (i.p.) injection of LPS (18 mg/kg) from Escherichia coli 0111: B4 (InvivoGen, tlr1-eb1ps) diluted in sterile normal saline. An equal volume of sterile normal saline was given to mice in the control group. Mice were monitored for signs of distress or discomfort. Eighteen hours after injection, rectal temperature was measured, and mice were euthanized by CO₂ asphyxiation for either bronchoalveolar lavage (BAL) or lung tissue collection. Mice that died before BAL and lung tissue collection (2 in myePoldip2^{+/+} group and 1 in myePoldip2^{-/-} group) were excluded. No difference between sexes was detected.

Bronchoalveolar lavage (BAL)

Mice were first euthanized by CO₂ inhalation and tracheas were exposed and cannulated using a 20-gauge lavage needle. For assessment of total cell counts in BAL, three lavages with 1 ml each of PBS containing 2 mM EDTA were injected in the tracheal lavage needle and recovered as previously described.²¹ The volume recovered was measured for normalization and then centrifuged at 300 g, 4°C for 10 min. Pellets were resuspended in Hank's balanced salt solution without Ca²⁺ and Mg²⁺ (HBSS-, Gibco, #14175) for either total BAL cell counts or flow cytometry. For total cell counting, pellets were processed with RBC lysis buffer (Alfa Aesar, #J62150) prior to counting using a Bio-Rad TC20 Automated cell counter.

Flow cytometry

For neutrophil identification in BAL, samples were processed with RBC lysis buffer right after collection and spun down at 300 g for 5 min at room temperature. The cell pellet was resuspended in HBSS containing 2 mM EDTA (RPI, #E14000) and cells were blocked with anti-mouse CD16/32 (ThermoFisher, #14-0161-82) for 15 min on ice, followed by incubation with anti-mouse antibodies on ice for 30 min in the dark. Antibodies were APC-Ly6G (ThermoFisher, #17-9668-82), eFluor450-CD11b (ThermoFisher, #48-0112-82), APC-eFluor780-CD45 (ThermoFisher, #47-0451-82). For evaluation of integrin surface expression, isolated neutrophils were labeled with eFluor450-CD11b or FITC-CD18 (Biolegend, #101405). For evaluation of L-selectin shedding, neutrophils were stained with CD62L (ThermoFisher, #11-0621-82). Flow cytometry was performed on a Cytex Aurora flow cytometer (Cytex Biosciences). Data were analyzed with Flowjo software (Tree star), and leukocytes were gated as CD45⁺; myeloid cells were further gated as CD11b⁺ and neutrophils were identified as Ly6G⁺. For complete blood cell counts, white blood cell differential counting was achieved using a Hemavet 1500 blood analyzer (CDC Technologies, Oxford, CT).

Immunofluorescence, histology and microscopy

Eighteen hours after PBS or LPS treatment, mice were sacrificed using CO₂ asphyxiation, and lungs were injected with 10% formalin through the trachea using a 21-gauge lavage needle. Lungs were then dissected, placed in 10% formalin for 24 h, and transferred to 70% ethanol, paraffin embedded and sectioned (5 μm). Fixed paraffin lung sections were used for hematoxylin & eosin (H&E) staining and immunostaining. For H&E staining, paraffin sections were deparaffinized then rehydrated in a series of xylene, ethanol and PBS. Hematoxylin and eosin staining were then performed according to standard protocols²⁴. Pictures were taken under a NanoZoomer-SQ Digital slide scanner (Hamamatsu) at 20X magnification. For immunostaining, 10 μg/ml proteinase K (Abcam, #ab64220) was applied for antigen retrieval (30 min, room temperature), and sections were blocked with 3% BSA containing 3% normal goat serum (Vector, #S-1000) prior to incubation with primary antibody against Ly6G (1:200 diluted, Abcam, #ab2557) overnight at 4°C. Sections were then stained with Alexa Fluor 568 goat anti-rat IgG (1:500 diluted, Invitrogen, #A11077), and mounted with vectashield mounting medium with DAPI (Vector, H-1200). Pictures were taken on a Zeiss LSM 800 Airyscan microscope at 20X magnification, and the ratio of Ly6G and DAPI positive area was calculated using ImageJ for assessment of neutrophil infiltration. Data were quantified from three fields of one section per animal, and 5 animals per group.

Bone marrow neutrophil isolation and purification

Primary bone marrow neutrophils were isolated as described²⁵ and purified by the immunomagnetic negative selection technique, using an Easysep Mouse Neutrophil Enrichment Kit (Stemcell Technologies, #19762). Briefly, both ends of the femur and tibia were dissociated after euthanasia and bone marrow cells were flushed using a 27-gauge needle and 10 ml syringe filled with HBSS- supplemented with 2% FBS (Benchmark, #100-106) and 2 mM EDTA. The cell suspension was passed through a 70 μm mesh nylon strainer to remove clumps of cells and debris and centrifuged at 300 g for 10 min. Resuspended cells were then processed following the manufacturer's instructions to get purified neutrophils. Neutrophil purity was always higher than 85%

and was assessed by staining with the fluorophore-labeled neutrophil marker, Ly6G, followed by flow cytometry analysis.

Cell culture

Primary rat pulmonary microvascular endothelial cells (RPMECs; Cell Biologics, #RN-6011) and primary mouse lung microvascular endothelial cells (MLMECs; Cell Biologics, #C57-6011) were cultured on plates pre-coated with 0.1% gelatin from bovine skin (Sigma; Cat No. G6650). Endothelial cell medium was supplemented with 2% fetal bovine serum, endothelial cell growth factors, and antibiotics (Cell Biologics; #M1266 for RPMECs, #M1168 for MLMECs). Cells were used from passage 4 to 6.

Static adhesion assay

Isolated bone marrow neutrophils were spun down at 300 g, 20°C for 5 min, resuspended in serum-free Dulbecco's Modified Eagle's Medium (DMEM; Sigma, #D5671) containing 0.2% BSA (Sigma, #3117332001), 2 mM L-glutamine (ThermoFisher, #25030), and Hoechst 33342 (1:2000, ThermoFisher, #62249), and incubated at 37°C, 5% CO₂ for 10 min. Cells were then washed twice with DMEM, and resuspended at 1x10⁶ cells/ml. MLMECs were seeded onto a 24-well plate and treated with 10 ng/mL TNF- α once a monolayer was formed. After 6 hours, MLMECs were washed twice with DMEM followed by addition of bone marrow neutrophils (2 x 10⁵ cell per well). Neutrophils and MLMECs were co-incubated for 30 min at 37°C followed by two washes with warm HBSS with Ca²⁺ and Mg²⁺ (HBSS+, Gibco, #14025) and then fixed using 3.7% paraformaldehyde (PFA, Electron Microscopy Science, #15714-S) for 10 min at room temperature. Fixed cells were washed twice with HBSS+ and immediately imaged with an Olympus IX71 inverted fluorescent microscope using the DAPI fluorescence channel at 10x magnification. Three representative pictures were taken per well, and triplicate wells were used for each condition. Images were analyzed with ImageJ software (NIH); stained neutrophil nuclei were counted using the "analyze particles" module to assess firm adhesion to the MLMEC monolayer.

μ -slide chemotaxis

μ -Slide Chemotaxis (ibidi GmbH, #80326) was used for the chemotaxis assay. Each slide contains three chambers, and each chamber consists of one channel for the cells and two reservoirs for the chemoattractant or chemoattractant-free media on either side of the channel. Prior to use, cell medium and μ -Slide were stored in the incubator at 37°C, 5% CO₂ overnight for equilibration. Poldip2^{+/+} and Poldip2^{+/-} bone marrow neutrophils were isolated as described above and incubated in HBSS+ containing Hoechst 33342 (1:2000) at 37°C for 10min, washed twice and then resuspended in HBSS+ at 3x10⁶ cells/ml before seeding into the central channel. Assays were conducted following the manufacturer's instructions. Briefly, the cell suspension (6 μ l) was seeded into the channel and the μ -slide was incubated inside a sterile Petri dish for 15 min with a wet tissue to minimize evaporation. Next, both reservoirs were filled with 65 μ L chemoattractant-free medium and then fMLP (final concentration 50 μ M) was added to one reservoir. Negative and positive control experiments were performed in the other two chambers of the same μ -slide, in which both reservoirs were filled with either chemoattractant-free medium or the same chemoattractant solution as in the chemotaxis experiments. Cell movement was observed using a Leica TCS SP5 II laser

scanning confocal microscope (Leica Microsystems CMS GmbH, Wetzlar, Germany). Time lapse videos were acquired using LAS AF software with a Plan-Neo 10× 0.3NA air objective. After adding 50 μ M fMLP, images were captured every minute for a total duration of 2 hours in brightfield mode and DAPI mode (using a 405 nm laser Diode 50 mW with a DAPI filter set). Cell trajectories were analyzed using a customized Python cell tracker software. Distance threshold was set as 30 μ m based on the cell trajectories of negative control experiments. Statistical significance ($P < 0.05$) was calculated from 3 independent experiments ($n = 3$) where over 60 cells were evaluated in each condition per experiment.

Transmigration assay

For the transmigration assay, 3.0 μ m pore size transwell membrane inserts were utilized. MLMECs (3×10^5) were seeded onto the membrane and after forming a monolayer at 24 hours, they were treated with 10 ng/ml TNF- α or media alone for 6 hours. Hoechst pre-stained neutrophils (0.5×10^6) were added to the upper chamber of each insert and 100nM fMLP or media alone was added to the lower chamber. After 2 hours of incubation at 37°C, non-migrated cells were removed from the upper surface using a wet cotton swab and migrated cells on the lower surface were fixed in 4% PFA for 3 min. Inserts were then washed 3 times with PBS and membranes were cut out from inserts and mounted on slides. Pictures were taken using an Olympus DP71 Digital Microscope at 10X and migrated neutrophils were counted by a blinded observer in six fields for each well using ImageJ software (NIH). Neutrophils transmigrated into the media were also collected and counted manually using hemocytometer.

Soluble ICAM-1 binding assay

The soluble ICAM-1 binding assay was used to assess beta integrin activation in neutrophils²⁶. Bone marrow cells were isolated from myePoldip2^{+/+} and myePoldip2^{-/-} mice and suspended in HBSS+. Cells were exposed to 2 mM EDTA (as negative control), 5 mM MnCl₂ (Sigma, #M1787) or an equal volume of HBSS+, in the presence of 10 μ g/ml recombinant mouse ICAM-1-Fc chimera (R&D Systems, # 796-IC-050) and 10 μ g/ml PE-conjugated anti-human IgG1 Fc (ThermoFisher, #12-4998-82) for 10 min at 37°C. Cells were fixed on ice with 3.7% PFA for 30 min and then labeled with APC-conjugated anti-Ly6G (ThermoFisher, #17-9668-82) to identify neutrophils. ICAM-1 binding was measured using flow cytometry measurement of PE mean fluorescence intensity in the neutrophil subset.

SYTOX Green assay

The SYTOX green assay was used to quantify the abundance of extracellular DNA as a surrogate of neutrophil extracellular trap (NET) formation as previously described.²⁷ Poldip2^{+/+} and Poldip2^{-/-} neutrophils were isolated as described above. Fifty thousand cells per well were plated in a 96 well black clear-bottom plate and incubated at 37°C for 1 h. Cells were then stimulated with 324 nmol of phorbol 12-myristate 13-acetate (PMA; Sigma, #P8139) or 50 μ g/ml of LPS (Sigma, #L4391). SYTOX green dye (5 μ M, Invitrogen, #S7020) was added to each well and the fluorescence was read with filter setting at 485-nm excitation/525-nm emission using a Synergy H1 Microplate Reader and Gene5 software (Biotek, Winooski, VT). Fluorescence was read every 15 min for a total of 90 min at 37°C. Four replicates were measured in each experiment. Three

independent experiments were performed. Both the time course curves, as well as final fluorescence at 90 min were analyzed.

Reactive oxygen species (ROS) production

Bone marrow neutrophils isolated from Poldip2^{+/+} and Poldip2^{+/-} mice were resuspended in HBSS+ and transferred to a 96 well plate (1x10⁶ neutrophils per well). A cytochrome C assay was applied for ROS production measurement.²⁸ Briefly, cytochrome C (100 nM) was added to all wells and 25 units of superoxide dismutase (SOD) was added to control wells. Neutrophils were stimulated with 100 nM PMA. Absorbance was read at 550 nm (absorbance of reduced Cytochrome C) and 490 nm (to control for non-specific absorbance) every minute for 2 hours immediately after application of PMA. The concentration of superoxide was calculated using the following formula $[O_2^{\cdot-} \text{ (nmol)}] = [(Abs(X)_{550} - Abs(X)_{490}) - (Abs(SOD)_{550} - Abs(SOD)_{490})] / (2.1 \times 10^4 \text{ M}^{-1} \text{ cm}^{-1} \times 0.294 \text{ cm}) \times 10^9 \times 10^{-4} \text{ L}$, where X is the well of interest, SOD the corresponding well containing superoxide dismutase, $2.1 \times 10^4 \text{ M}^{-1} \text{ cm}^{-1}$ is the Cytochrome C extinction coefficient, 0.294 is the distance travelled by light (cm), 10^{-4} L is the reaction volume and 10^9 is the conversion coefficient from mol to nmol. The average of 3 independent experiments (2-6 independent wells each) was calculated.

RNA extraction and RT-qPCR

Total RNA was purified with Qiazol (Qiagen, #79306) and the RNeasy Plus kit (Qiagen, #74104). Reverse transcription was performed using Protoscript reverse transcriptase (New England Biolabs) with random primers. The resulting cDNA was amplified with previously validated primers against ribosomal protein L13A (RPL), Hypoxanthine Phosphoribosyl transferase (HPRT), Interleukin 1 Beta (IL-1 β), Interleukin 6 (IL-6), Tumor Necrosis Factor Alpha (TNF- α), C-C Motif Chemokine Ligand 2 (CCL-2/MCP-1), C-X-C Motif Chemokine Ligand 1 (CXCL-1), C-X-C Motif Chemokine Ligand 2 (CXCL-2), and Poldip2 (for primer details please refer to Table 1). RPL and HPRT were used as housekeeping genes as their expression was not affected by LPS treatment. Note that Poldip2 primers can detect messages transcribed from both floxed and Cre-excised alleles. Amplification was performed in 96-well plates using Forget-Me-Not EvaGreen qPCR Master Mix with low ROX (Biotium, #31045) in a QuantStudio 7 instrument (Invitrogen). Data analysis was performed using the mak3i module of the qpcR software library (version 1.4-0)^{29,30} in the R-environment.³¹ Final result quantification was expressed in arbitrary units.

Enzyme-linked immunosorbent assay (ELISA)

Bone marrow neutrophils isolated and purified from myePoldip2^{+/+} and myePoldip2^{+/-} mice were plated on 24-well plate (3×10^6 /600 μ L/well) and stimulated with LPS (1 μ g/ml) or media only for 8 hours at 37°C, 5% CO₂. Supernatant was then collected for TNF- α , IL-1 β , and IL-6 production quantification. Commercial ELISA kits (R&D, #MLB00C, #M6000B, #MTA00B) were utilized according to the manufacturer's instructions. Five independent experiments were performed, and two replicates were measured in each experiment.

Western blotting

Whole cell lysate was prepared from isolated neutrophils using a lysis buffer described in our previous study:²⁰ 0.3 M NaCl, 0.2% SDS, 0.1 M Tris base, 1% Triton X-100, 10 µg/ml aprotinin, 10 µg/ml leupeptin, 1 mM PMSF, and Halt phosphatase inhibitor cocktail (ThermoFisher, #78428). Homogenates were centrifuged at 12,000 g at 4°C for 10 min and brought to equal concentration in Laemmli buffer before boiling at 100°C for 10 min. For Pyk2 phosphorylation detection, bone marrow neutrophils were plated onto ICAM-1 coated 6-well plates and stimulated with TNF-α or media alone for the specified time. Neutrophil lysates were then prepared by adding 2x laemmli buffer and boiling for another 5 min. Samples were stored at -20°C until gel loading. Proteins were separated by SDS-PAGE, transferred to nitrocellulose membranes (GE, #10600003) and assessed by blotting with primary antibodies against Poldip2 (Abcam, #ab181841), Pyk2 (CST, #3292S), phosphorylated Pyk2 (CST, #3291S), β-actin (CST, #4970) and vinculin (Sigma, #V4505). Blots were incubated with horseradish peroxidase (HRP)-conjugated secondary antibodies [anti-mouse (GE, NA931V) and anti-Rabbit (Cell signaling technology, #70745)]. Detection was performed using enhanced chemiluminescence (ThermoFisher, #32106) and autoradiography film (Genesee scientific, # 30-810L). Detected bands were scanned using an Epson Perfection V800 Photo scanner, and densitometry was performed using ImageJ.

Statistical Analysis

Analyses were carried out using results from 3-10 independent experiments with GraphPad Prism software version 8. Data were represented as medians with their 95% confidence intervals (CI) and analyzed using non-parametric methods, either Mann Whitney or Kruskal-Wallis with Dunnett multiple comparisons. A threshold of $P < 0.05$ was considered significant. Micrographs showing average numbers of adherent cells were selected as representative.

Table S1. Major Resources Table - Wild Type and Genetically Modified Animals (in vivo studies).

Species	Vendor or Source	Background Strain	Sex	Persistent ID / URL
Mouse	The Jackson Laboratory	C57BL/6J	Both	https://www.jax.org/strain/000664
Mouse	The Jackson Laboratory	C57BL/6	Both	https://www.jax.org/strain/004781
Mouse	Griendling, K.K.	C57BL/6	Both	https://doi.org/10.1371/journal.pone.0247261
Mouse	TIGM	C57BL/6	Both	https://tigmtrack.tamu.edu/tigm-web/pages/publicSearchResult.xhtml?type=%27Gene%27&name=%27Poldip2%27

Antibodies

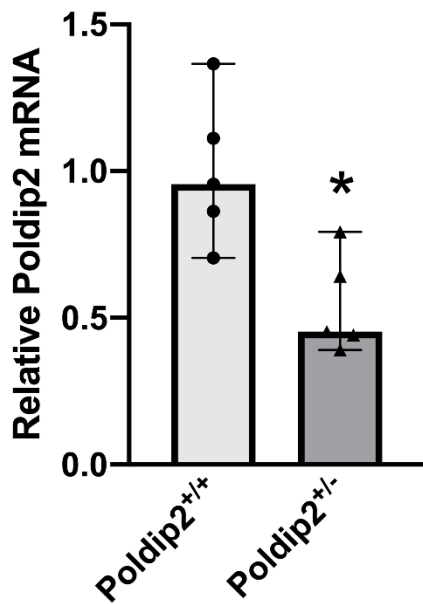
Target antigen	Vendor or Source	Catalog #	Working concentration	Lot # (preferred but not required)	Persistent ID / URL
Ly6G (Flow cytometry)	ThermoFisher	17-9668-82	1:100		
CD11b (Flow cytometry)	ThermoFisher	48-0112-82	1:100		
CD45 (Flow cytometry)	ThermoFisher	47-0451-82	1:100		
CD18 (Flow cytometry)	Biolegend	101405	1:100		
CD62L (Flow cytometry)	ThermoFisher	11-0621-82	1:100		
Ly6G (Immunofluorescence)	Abcam	ab2557	1:200		
Biotinylated Rat IgG	Vector	BA-9400	1:400		
Human IgG1 Fc (Flow cytometry)	ThermoFisher	12-4998-82	10 µg/ml		
Poldip2	Abcam	Ab181841	1:2000		
β2-integrin	R&D system	AF1730	1:2000		
Vinculin	Sigma	V4505	1:2000		
Phospho-Pyk2 (Tyr402)	Cell signaling technology	3291S	1:1000		
Pyk2	Cell signaling technology	3292S	1:2000		
β-actin	Cell signaling technology	4970	1:5000		

Mouse IgG	GE	NA931V	1:2000		
Rabbit IgG	Cell signaling technology	70745	1:5000		

Cultured Cells

Name	Vendor or Source	Sex (F, M, or unknown)	Persistent ID / URL
Mouse primary lung microvascular endothelial cell	Cell biologics	unknown	C57-6011
Rat primary lung microvascular endothelial cell	Cell biologics	unknown	RN-6011

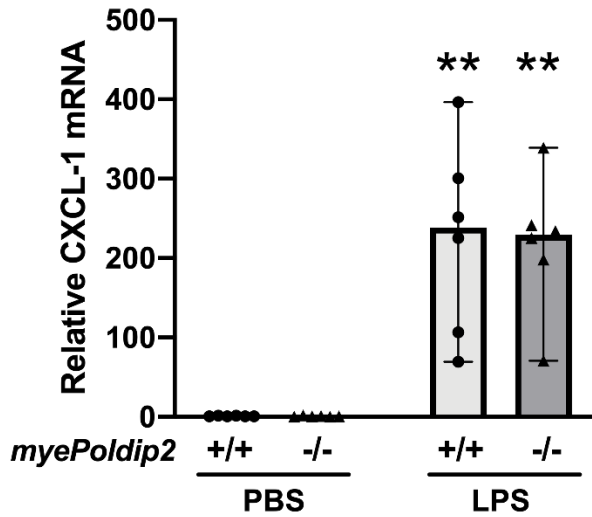
Figure S1. Poldip2 expression in Poldip2^{+/-} mice.



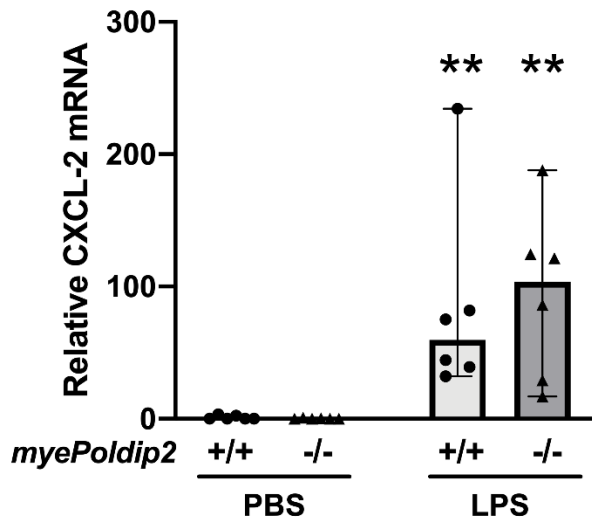
Poldip2 mRNA expression (normalized to RPL and HPRT) in purified neutrophils measured by quantitative RT-PCR. Data represent medians with 95% confidence intervals (n=5); * P<0.05 (Mann Whitney test). Poldip2 indicates polymerase (DNA-directed) delta interacting protein 2; RPL, ribosomal protein L13A; HPRT, hypoxanthine guanine phosphoribosyl transferase; and RT-PCR, real time polymerase chain reaction.

Figure S2. Poldip2 knockdown in myeloid cells does not affect LPS-induced upregulation of neutrophil-targeting chemokines in mouse lung.

A

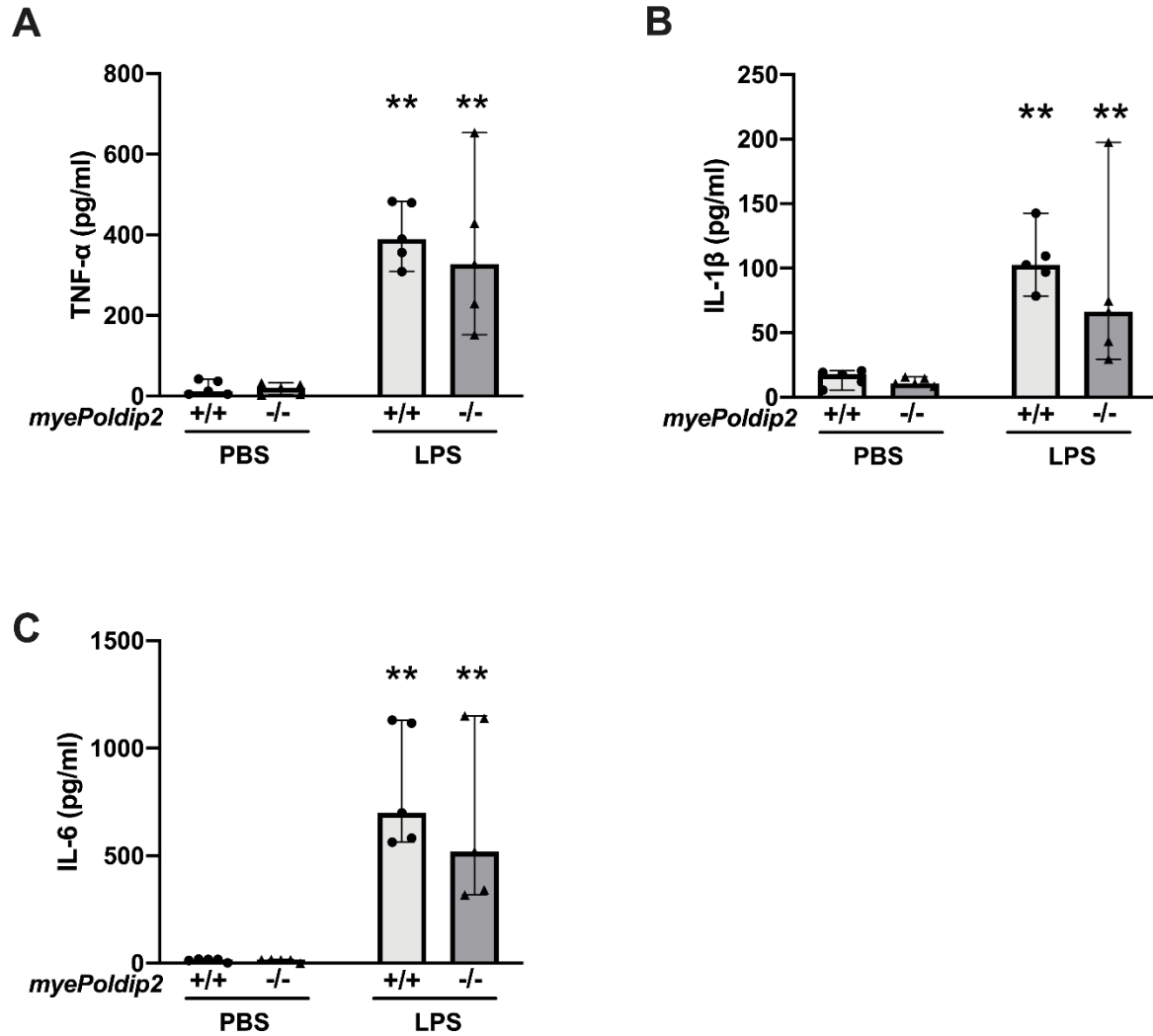


B



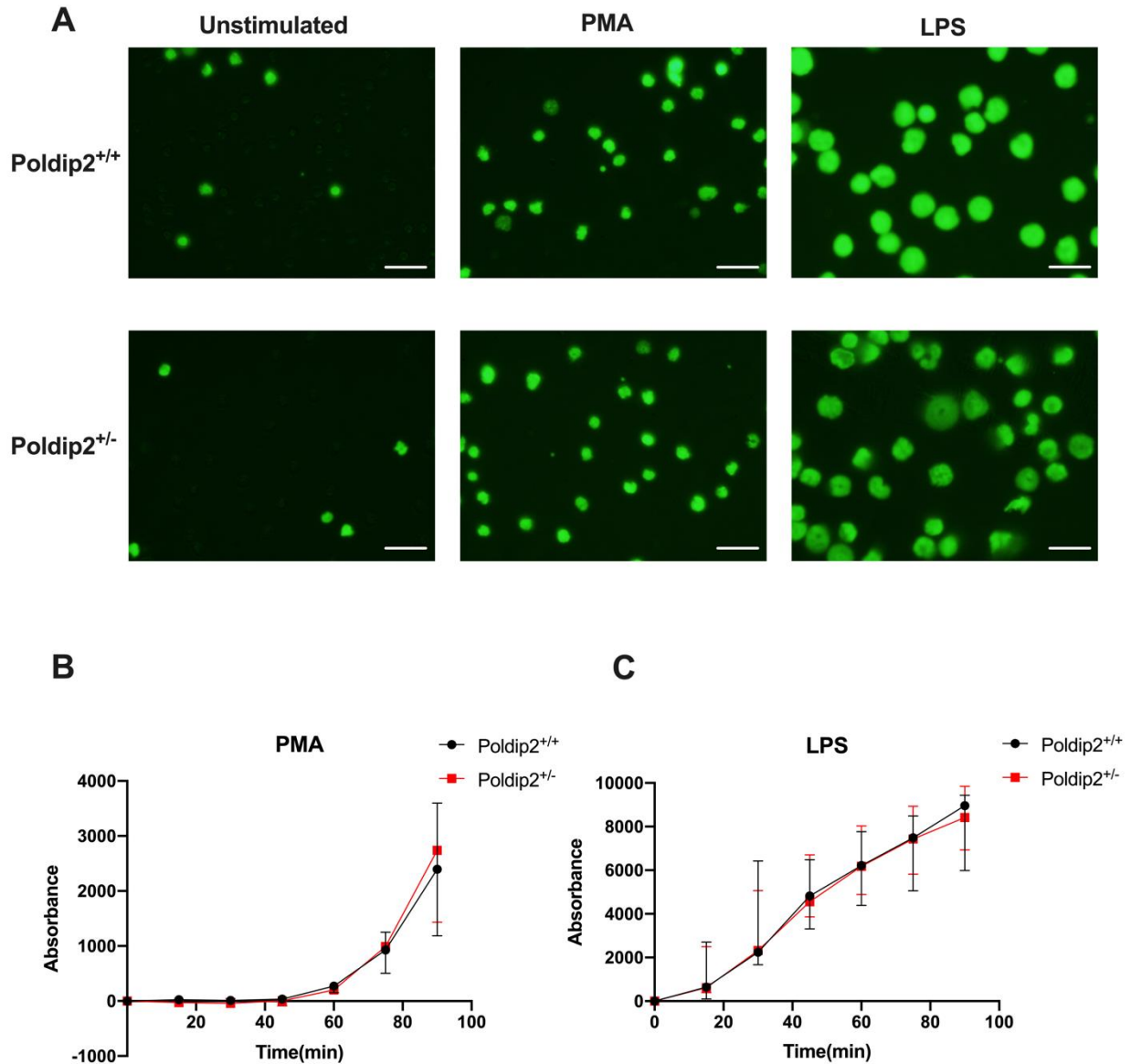
A-B. Intraperitoneal administration of LPS (18mg/kg) induced a significant increase at 18 hours in mRNA expression of chemokines CXCL-1 (A) and CXCL-2 (B) in lung. Data represent medians with 95% confidence intervals (n=6); ** P<0.01 compared to the PBS group of the same genotype (Mann Whitney tests). There was no significant difference between genotypes within the PBS and LPS groups. Poldip2 indicates polymerase (DNA-directed) delta interacting protein 2; PBS, phosphate buffered solution; LPS, lipopolysaccharide; CXCL-1, chemokine (C-X-C motif) ligand 1; and CXCL-2, chemokine (C-X-C motif) ligand 2.

Figure S3. Quantification of pro-inflammatory cytokines released by LPS stimulated neutrophils.



Isolated bone marrow neutrophils from *myePoldip2*^{+/+} and *myePoldip2*^{-/-} mice were cultured in RPMI 1640 and stimulated with LPS (1 μ g/ml) or media alone for 8 hours. Cell supernatant was then collected for TNF- α (A), IL-1 β (B) and IL-6 (C) production. Data represent medians with 95% confidence intervals (n=5), ** P<0.01 compared to the PBS group of the same genotype (Mann Whitney tests). Poldip2 indicates polymerase (DNA-directed) delta interacting protein 2; LPS, lipopolysaccharide; TNF- α , tumor necrosis factor α ; IL-1 β interleukin-1 β ; and IL-6, interleukin-6.

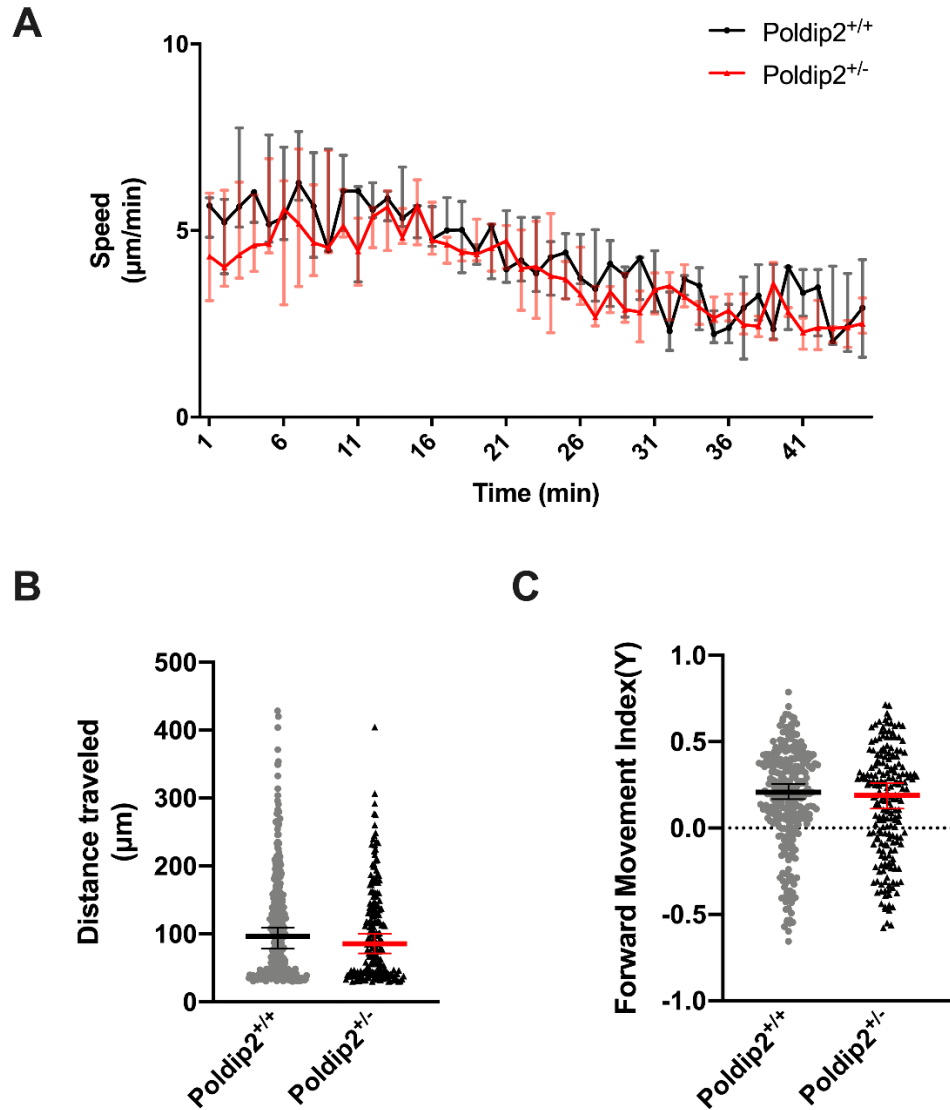
Figure S4. NET production in response to PMA and LPS stimulations.



A. Representative pictures of NET formation at 90 min under different conditions.

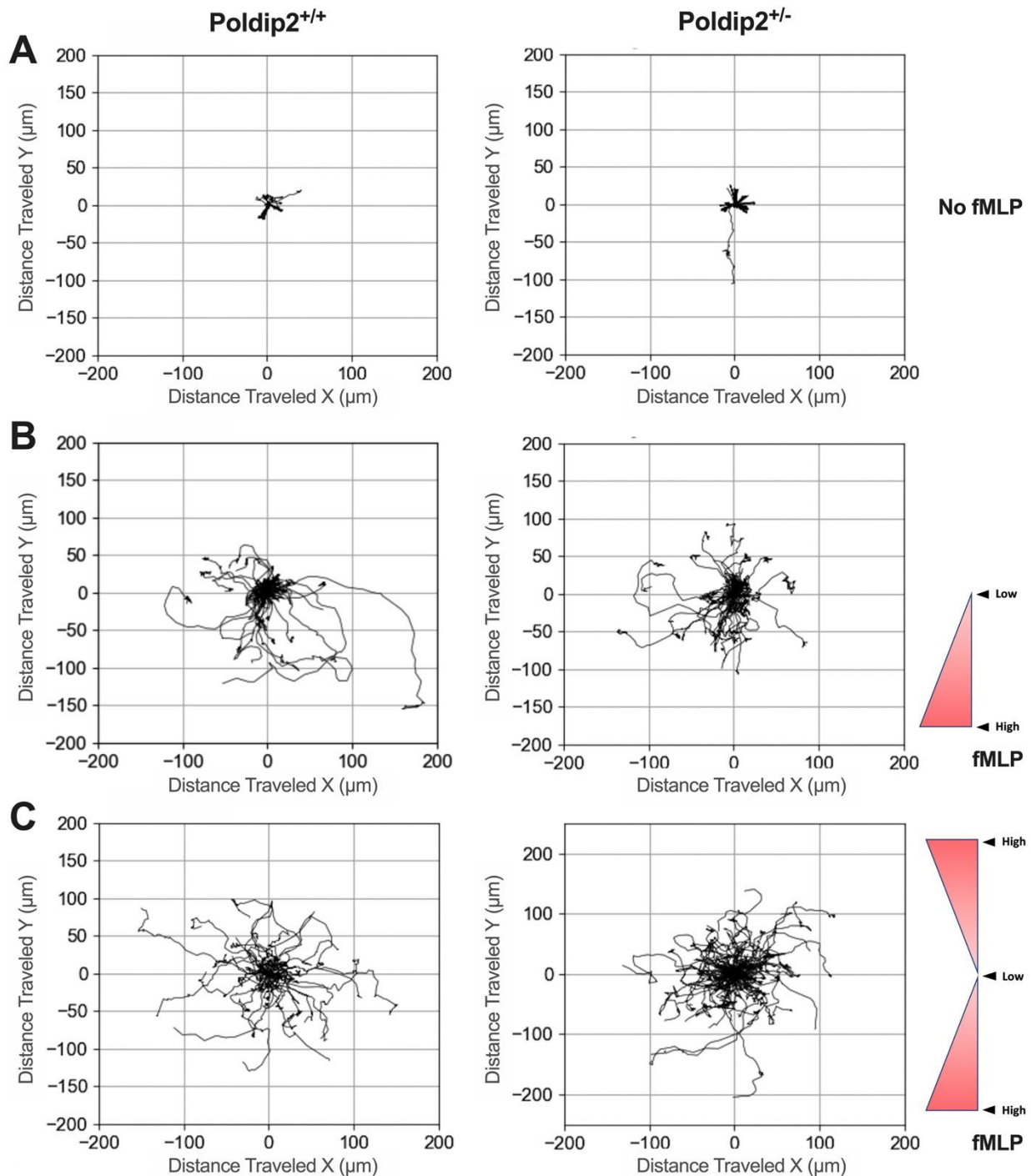
B-C. Neutrophils isolated from Poldip2^{+/+} and Poldip2^{+/-} mice were stimulated with 324 nM PMA (B) or 50µg/ml LPS (C), and fluorescence intensity was recorded for 90 min. Scale bars represent 50µm. Error bars represent medians with 95% confidence intervals (n=3). There was no significant difference between genotypes. NET indicates neutrophil extracellular trap (NET); Poldip2, polymerase (DNA-directed) delta interacting protein 2; PMA, phorbol 12-myristate 13-acetate; and LPS, lipopolysaccharide.

Figure S5. Poldip2 knockdown does not affect neutrophil motility.



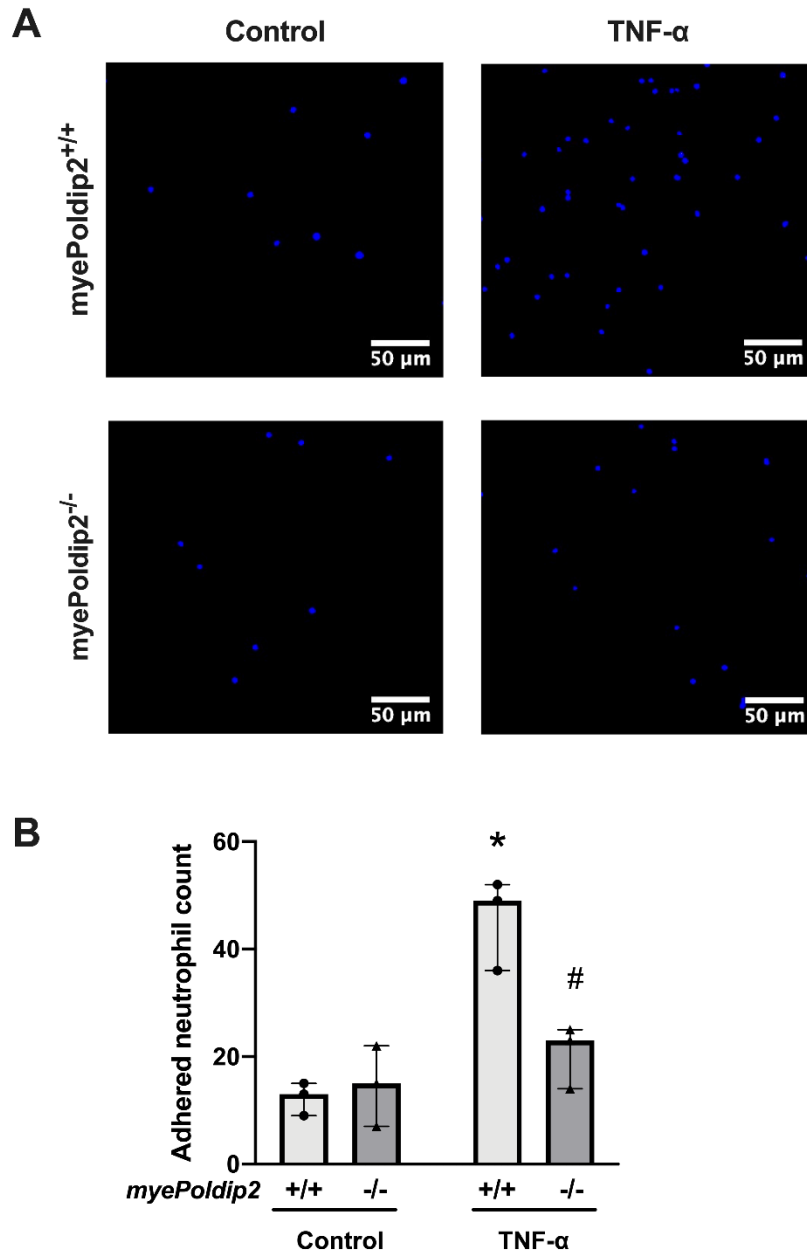
A-C. Isolated bone marrow neutrophils were seeded into μ -slides with 50 μM fMLP on one side. Photomicrographs of neutrophils isolated from Poldip2^{+/+} and Poldip2^{+/-} mice were taken every minute for a period of 45 minutes, starting immediately after plating. The paths of more than 60 neutrophils were recorded in each experiment and 3 independent experiments were performed. (A) Migration speed as a function of time; (B) Total distance traveled; (C) Forward movement index [FMI(Y)] toward fMLP, calculated as Y axis fraction of total distance traveled for 45 min. Single dots represent distance traveled by single cells, lines and error bars represent medians with 95% confidence intervals (n=3), no significant difference was observed between genotypes. Poldip2 indicates polymerase (DNA-directed) delta interacting protein 2; and fMLP, N-formylmethionyl-leucyl-phenylalanine.

Figure S6. Trajectories of fMLP-stimulated neutrophils.



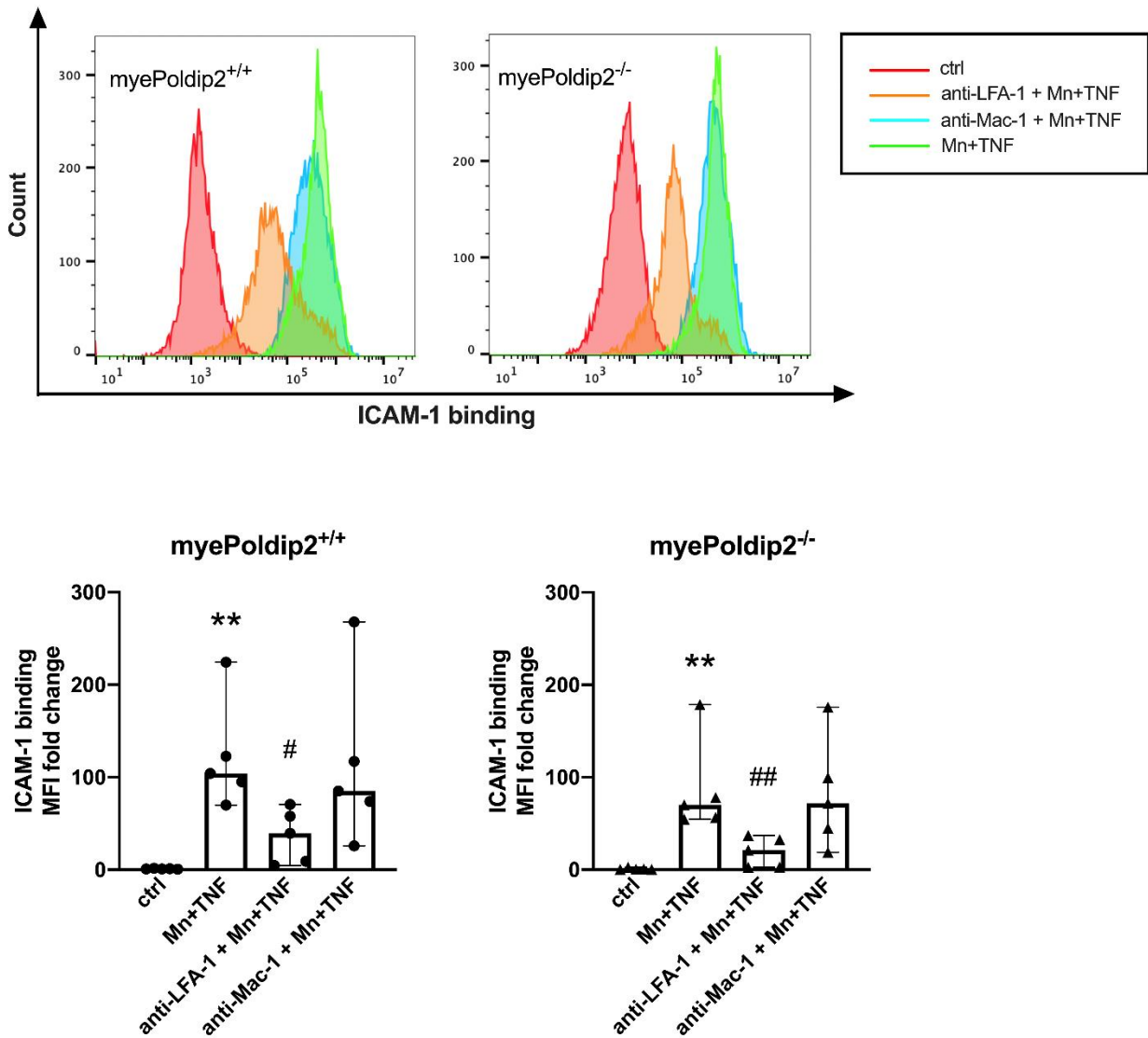
A-C. Representative cell trajectories of bone marrow neutrophils isolated from *Poldip2*^{+/+} and *Poldip2*^{+/-} mice, recorded for 45 minutes upon seeding. There was no significant difference in motility between genotypes in response to media alone (A), fMLP (50µM) on one side (B) and fMLP (50µM) on both sides of the assay chamber (C). *Poldip2* indicates polymerase (DNA-directed) delta interacting protein 2; and fMLP, N-formylmethionyl-leucyl-phenylalanine.

Figure S7. Poldip2 knockdown impairs neutrophil firm adhesion.



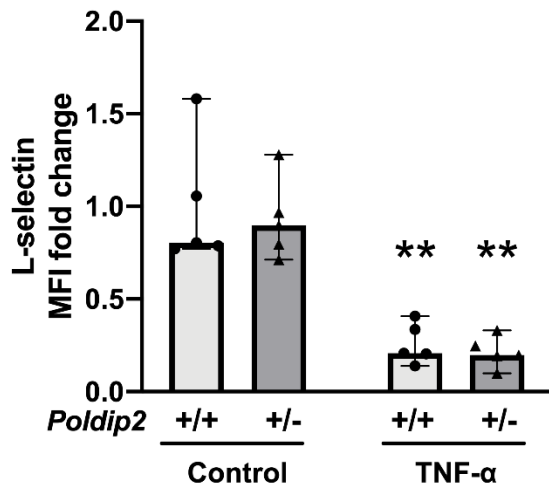
A. Representative pictures of neutrophil adhesion to RPMEC monolayer. Firm adhesion to TNF- α stimulated endothelial monolayers was significantly impaired in myePoldip2^{-/-} neutrophils. **B.** Quantification of results from panel A. Data represent adhered neutrophils relative to control as medians with 95% confidence intervals (n=3); * P<0.05 compared to myePoldip2^{+/+} control group, # P< 0.05 compared to myePoldip2^{+/+} TNF- α group (Mann Whitney tests, one tailed). Poldip2 indicates polymerase (DNA-directed) delta interacting protein 2; RPMEC, rat pulmonary microvascular endothelial cell; and TNF- α , tumor necrosis factor α .

Figure S8. Soluble ICAM-1 binding with LFA-1 or Mac-1 blocking antibody.



Neutrophils isolated from *myePoldip2*^{+/+} and *myePoldip2*^{-/-} mice were incubated with either LFA-1 blocking antibody, Mac-1 antibody or HBSS (without Ca²⁺ and Mg²⁺) prior to Mn²⁺ and TNF stimulation. ICAM-1 binding was quantified by mean fluorescence intensity (MFI). In both genotypes, an apparent decrease of ICAM-1 binding can be identified after blocking LFA-1, which was not observed with Mac-1 blockade. Bar graphs represent medians with 95% confidence intervals (n=5), ** P<0.01 compared to control, # P<0.05, ## P<0.01 compared to Mn+TNF (Mann Whitney tests). Poldip2 indicates polymerase (DNA-directed) delta interacting protein 2; Mn, manganese chloride; LFA-1, integrin alpha L; Mac-1, integrin alpha M; HBSS, Hanks balanced salt solution; TNF, tumor necrosis factor α ; and ICAM-1, intercellular adhesion molecule 1.

Figure S9. L-selectin shedding in response to TNF- α stimulation.



Isolated bone marrow neutrophils were incubated with 20ng/ml TNF- α or media alone for 1 hour. Cells were then labeled with FITC-L-selectin antibody. Data represent fluorescence intensity (MFI) fold change as medians with 95% confidence intervals (n=5); ** P<0.01 compared to the control group of the same genotype (Mann Whitney tests). No significant difference was noted between genotypes. Poldip2 indicates polymerase (DNA-directed) delta interacting protein 2; and TNF- α , tumor necrosis factor α .